

## Quantification and reduction of power peaks in railway networks: a simulation-based approach

Daniel Regueiro Sánchez

Master Thesis

Civil Engineering

July 2021

## Acknowledgements

With the completion of this thesis, six years of university studies devoted to civil engineering come to an end. It is hard not to reflect on what has been a truly exciting, intense and enriching journey. I feel very grateful for having had the opportunity to spend an exchange year at ETH Zurich and carrying out my Master Thesis at the IVT has been a great way to finalize my studies. The last four months working on this project have been demanding as well as stimulating, and many people have contributed in one way or another towards the successful completion of this work.

First and foremost, I would like to express my most sincere gratitude to Prof. Dr. Francesco Corman for agreeing to supervise this thesis, for his willingness to help with all the necessary arrangements since our first contact before I even moved to Zurich, and for his guidance throughout the course of the project. My deepest appreciation also to Michael Nold, for the daily supervision and for his support in the countless meetings we held during the last months.

I also wish to thank my friends from my home university, who regularly showed interest in my work and were an essential support during this year abroad. Very specially, I want to thank Agustín Sánchez-Arcilla for his suggestions and for always transmitting me the right motivation to be able to finish this thesis successfully.

I would also like to mention the friends I met in Zurich during this academic year and who have made my stay abroad a truly remarkable experience.

Last but not least, my greatest appreciation goes to my parents Ana María and Benito. Thanks for your unconditional support and for giving me the necessary encouragement in the moments when I needed it the most.

I wish to extend my appreciation to my grandma Pepita, and to all other family members, friends and classmates who were at some point interested in my work.

*Daniel Regueiro Sánchez*

Zurich, July 2021

Master Thesis

# Quantification and reduction of power peaks in railway networks: a simulation-based approach

Daniel Regueiro Sánchez  
IVT ETH Zurich  
Stefano-Franscini-Platz 5, 8093 Zurich, Switzerland

Phone: +34 669 586 327  
E-Mail: drs97@outlook.es

July 2021

## Abstract

Power peaks are an undesirable phenomenon which unavoidably occurs in railway operations due to the inharmonious movement of trains. Under severe delays, power peaks can reach extremely high values putting too much pressure into the power grid, even leading to a blackout. In this paper, a railway simulation tool is developed based on timetable and energy consumption data for the quantification of the power peaks in a railway network. It is verified how impunctuality issues during operation can lead to very high peak values of the overall power demand. Additionally, and in order to mitigate the power peaks, different operational measures are implemented to optimize the power demand profile of the railway network. This is performed following a two-fold optimization strategy which includes both shifting the departure times of trains and the limitation of their maximum traction power between two stations. The implemented simulation-based optimization shows great potential to reduce the power peaks, particularly by means of limiting the maximum traction power of the trains.

## Keywords

Power peaks; Railway simulation; Optimization; Departure delays; Traction power limitation; Timetable variation; Energy management

## Preferred citation style

Regueiro Sánchez, D. (2021) Quantification and reduction of power peaks in railway networks: a simulation-based approach, *Master thesis*, IVT, ETH Zurich, Zurich.

## Table of contents

1	Introduction.....	1
1.1	Power peaks in railway operations .....	1
1.2	Aim and objectives .....	2
1.3	Thesis outline.....	3
2	Literature review .....	5
2.1	Simulation of railway networks.....	5
2.2	The energy efficient train control problem and other related energy optimization problems .....	7
2.3	Approaches and formulations for the reduction of power peaks in railway networks ....	10
2.4	Research gap and contribution of this thesis .....	14
3	Development of a simulation tool for the quantification of the power consumption of trains in a railway network .....	15
3.1	Case study: The canton of Ticino in Switzerland.....	15
3.2	Simulation inputs.....	18
3.3	The simulation .....	20
3.4	Simulation outputs.....	24
4	Delays, timetable variation and stochastic effects .....	29
4.1	Delay scenarios considered .....	29
4.2	Results and discussion .....	32
5	Simulation-based optimization of train runs and reduction of power peaks .....	47
5.1	Modification of the departure time of trains.....	47
5.2	Limitation of the maximum traction power of trains .....	48
5.3	Optimization procedure .....	51
5.4	Results and discussion .....	56
6	Conclusions and outlook.....	67
7	Reference list .....	69

## List of tables

Table 1: Train lines departing from Locarno .....	15
Table 2: Train lines departing from Luino .....	16
Table 3: Rolling stock considered in the simulation .....	17
Table 4: Power peak and other indicators using rolling averages .....	25
Table 5: Summary of results of all delay scenarios for the power peak .....	46
Table 6: Results of the power demand optimization with an objective power of 10000 kW ..	57
Table 7: Decision variables corresponding to optimization 1 .....	58
Table 8: Decision variables corresponding to optimization 2 .....	58
Table 9: Results of the power demand optimization with an objective power of 8000 kW ....	60
Table 10: Decision variables corresponding to optimization 5 .....	60
Table 11: Results of the power demand optimization with an objective power of 8000 kW (including delays) .....	62
Table 12: Decision variables corresponding to optimization 1 .....	63
Table 13: Decision variables corresponding to optimization 2 .....	64

## List of figures

Figure 1: Typical speed profile and associated energy consumption .....	8
Figure 2: Railway lines in the Canton of Ticino, updated 2021 after the opening of the Ceneri base tunnel .....	16
Figure 3: SBB Re 460 locomotive (left) and TiLo Flirt RABe 524 regional train (right) .....	17
Figure 4: Considered network with block sections and delimitation of the power supply area .....	18
Figure 5: Graph representation of the railway network .....	19
Figure 6: Schematic summary of the simulation inputs and outputs .....	20
Figure 7: Detail of the block sections and signaling at the stations .....	21
Figure 8: Possible driving schemes between two signals .....	22
Figure 9: Flowchart summarizing the logic of the simulation .....	23
Figure 10: Power demand profile during the simulation horizon .....	24
Figure 11: Power peaks using different rolling averages .....	26
Figure 12: Train trajectories during the simulation horizon .....	28
Figure 13: Probability density functions of some of the delay distributions used .....	30
Figure 14: Interface between the power supply area and the rest of the railway network .....	31
Figure 15: Results of delay scenario 1 (power peak) .....	32
Figure 16: Results of delay scenario 1 (90 <sup>th</sup> perc. power) .....	33
Figure 17: Results of delay scenario 1 (50 <sup>th</sup> perc. power) .....	33

Figure 18: Distribution of the actual departure delays of train from lines S 20 and S 30..... 35

Figure 19: Power demand profile during the simulation horizon (delay scenario 1)..... 35

Figure 20: Train trajectories during the simulation horizon (delay scenario 1)..... 36

Figure 21: Results of delay scenario 2 (power peak) ..... 39

Figure 22: Results of delay scenario 2 (90<sup>th</sup> perc.power)..... 39

Figure 23: Results of delay scenario 2 (50<sup>th</sup> perc. power)..... 40

Figure 24: Train trajectories during the simulation horizon (delay scenario 2)..... 42

Figure 25: Results of delay scenario 3 ..... 43

Figure 26: Comparison of power peak distribution in delay scenario 3 ..... 44

Figure 27: Difference between power limitation and speed reduction ..... 48

Figure 28: Power limitation and its effect on the velocity-force diagram ..... 49

Figure 29: Effect of power limitation on the speed profiles of trains ..... 50

Figure 30: Time-power, distance-power, time-distance and distance-velocity diagrams..... 50

Figure 31: Optimization strategy..... 53

Figure 32: Flowchart describing the optimization procedure ..... 55

Figure 33: Optimized power profile (optimization 5)..... 61

Figure 34: Comparison of the power consumption histograms corresponding to the original and optimized power profiles ..... 61

Figure 35: Comparison of both optimized power demand profiles ..... 65

Figure 36: Optimized power profile (optimization 1, including delays)..... 66

Figure 37: Comparison of the power consumption histograms corresponding to the original and optimized power profiles (optimization 1, including delays)..... 66

# 1 Introduction

## 1.1 Power peaks in railway operations

The power supply of a railway network is typically divided into smaller electric substations. Each electric power supply substation of the railway system delivers the electric power to a part of the railway network. Inside this part of the railway network, there are several trains in operation. During the railway operations, each train receives power from the electric power supply station and delivers power back by means of electric regenerative braking. Due to this railway operation, the delivered power from the power supply station is not constant. Actually, it is extremely varying in time and has power peaks.

The power peaks are critical for the railway operator and the system availability. Each power supply is constructed for certain strength of power consumption peaks. If the peaks are higher, the entire power supply system can fail with the result of a blackout in the considered railway network part.

The *normal power consumption*  $P_{norm}(t)$  in the considered network part is the summation of the power consumption of the individual trains (1):

$$P_{norm}(t) = \sum_{i=1}^{n_{trains}} P_i(t) \quad (1)$$

The power peak is defined as the maximal value that the normal power consumption achieves (2). Normally, a specified time horizon  $T$  is considered and power consumption is considered for instances that are  $\Delta_t = 1$  second long.

$$P_{norm.max} = \max_{T, \Delta_t} \left( \sum_{i=1}^{n_{trains}} P_i(t) \right) \quad (2)$$

The *theoretical maximum power consumption* ( $P_{theoretical.max}$ ) is the summation of the maximum power consumption of each vehicle in the railway network part considered (3):

$$P_{theoretical.max} = \sum_{i=1}^{n_{trains}} \max_{T, \Delta_t} P_i(t) \quad (3)$$

The *normal power consumption* in the railway network part is much lower than the *theoretical maximum power consumption*, due to the fact that in real railway operations each vehicle does not consume its maximum power at the same time. The *maximal power supply capability* ( $P_{supply.max}$ ) of the power supply station is typically larger than the *normal maximal power consumption* but lower than the *theoretical maximum power consumption* (4):

$$P_{norm}(t) \leq P_{norm.max} < P_{supply.max} < P_{theoretical.max} \quad (4)$$

Under smooth operations, and since timetables are already strategically designed to avoid excessive power peaks, inequality (4) holds. However, under some delays or under other disruptions, the *normal maximal power consumption* can exceed the *maximal power supply capability*, with the risk of causing a blackout. By conducting a timetable simulation of the considered railway network part, the *normal maximal power consumption* can be computed and the conditions under which the power peaks reach extremely high values determined.

## 1.2 Aim and objectives

There are fundamentally two aims in this project, as the title of thesis suggests. On the one hand, the quantification of the power peaks in a railway network. This includes both the quantification of the power peaks when following the normal timetable operation, and also the cases with departure delays at the stations. For this purpose, a simulation tool is to be developed to allow for the detailed representation of train movements and their power consumption. The objectives of this part of the work include the development of the aforementioned simulation tool, which shall use predetermined power consumption profiles together with timetable information to determine the normal power consumption in the network and its power peak. The tool shall be kept generic, i.e., it should be easily adaptable to other networks or operational conditions. Additionally, the tool shall be capable of introducing delays in the simulation to study the associated stochastic effects and the alteration of the power demand profile under impunctuality conditions.

On the other hand, and constituting the second aim of the thesis, is the reduction of the power peaks obtained through the simulation. By implementing different operational measures (mainly by shifting the departure times of trains at stations and by limiting the power

consumption in some sections) the power demand profile shall be optimized, such that the maximal power consumption during the planned time horizon is kept below an objective value to be set. Other objectives include the analysis of the trade-off incurred in the optimization by analyzing the additional delay of the trains, as well as determining the most efficient ways to avoid the power peaks. Optimizations are to be performed both in cases with normal timetable operation and in cases including stochastic delays.

### 1.3 Thesis outline

The thesis is structured in three main chapters, following the two main aims described in section 1.2. The first aim, constituting the development of the timetable simulation tool, is split into two independent chapters: one including the description of the simulation itself, and a second chapter with the inclusion of delays in the simulation. The third main chapter includes the optimization procedure leading to the reduction of power peaks. Naturally, an extensive literature review is included and the thesis finalizes with the conclusions drawn from the study and suggested future research.

- **Chapter 1: Introduction.** Includes some background and motivation on the project, as well as the aim and objectives to be accomplished.
- **Chapter 2: Literature review.** Includes an extensive review on research trends covering simulation models for railway operations, typical energy optimization problems and formulation and approaches for power peak reduction in railway networks.
- **Chapter 3: Development of a simulation tool for the quantification of the power consumption of trains in a railway network.** Describes the development the simulation tool, including the case study which has been considered, the inputs and outputs of the simulation and the actual functioning of the tool.
- **Chapter 4: Delays, timetable variation and stochastic effects.** Includes the description of the different delays scenarios that have been considered, as well as the presentation of the obtained results and their discussion commenting on the changes in the power consumption profile under stochastic delays.

- **Chapter 5: Simulation-based optimization of train runs and reduction of power peaks.** Includes the description of the logic behind the optimization procedure, the potential of the approach and assumptions which are exploited, as well as the presentation of optimization the results and their discussion.
- **Chapter 6: Conclusions and outlook.** The final conclusions of the study (covering both the quantification of the power peaks and their reduction) are presented together with future suggestions and improvements.

## 2 Literature review

### 2.1 Simulation of railway networks

Computer simulations have been widely used since the late 20th century for the modelling and research of many aspects concerning railway networks. The recent advances both in hardware and software technologies have allowed for the development of more advanced, detailed and precise simulation frameworks which have facilitated the research and optimization of railway systems from very different perspectives. Simulation models are nowadays widely used for capacity studies, timetabling optimization, signalling studies, power supply and traction equipment studies, delay propagation, among others (Ho *et al.*, 2002).

Typically, railway simulation models are delimited into two large groups when it comes to determining the way in which train movements are computed: time-based and event-based models (Goodman *et al.*, 1998). Time-based models resemble a microsimulation, where the position and all other attributes of the trains are updated at each time step. The precision of these models is typically very high, although they must cope with a very high computational demand. This can be alleviated by increasing the time step of the simulation, although then the precision of the simulation may be compromised.

On the other hand, event-based models only update the different attributes of the simulation in case an *event* happens, instead of being continuously updated every given time step. An event is typically defined as the arrival or departure of a train from a station, a train moving from a block section to the next, etc. Commonly, one event triggers a posterior event since different trains are usually connected by means of different conflicts or interactions which may occur in the network. Consequently, the simulation is only updated after each of the predefined events, and the exact position of trains may remain unknown. Only the occupied block sections or stations are determined with certainty. Event-based models are also very popular, due to their lower computational complexity which allows for larger-scale simulation and studies in a reasonable simulation time.

Goodman *et al.* (1998) affirm that time-based models are solely justified in case where details of the exact movements of the trains are needed, such as for energy consumption or signaling

design studies. In this paper, a new approach using an event-based simulation with predefined train trajectories and associated energy consumptions will be used to compute the energy consumption of trains, therefore overcoming the drawback of the high computational cost required in time-based simulations.

The considerations regarding the signaling system to be used in the simulation framework are extremely important. Traditionally, only fixed block signaling was included in simulations (Ho *et al.*, 2002). However, with advances in computation, most simulations also allow for the usage of moving-block signaling, meaning that block section are defined based on the current location of the trains, instead of being predetermined beforehand (Hill, 1995).

The selected signaling system is also crucial for the modelling of train conflicts and interactions at the junctions and intersections of the networks, as argued by Ho *et al.* (1995). In their paper, they use pre-calculated run-times of trains to determine the events in their event-based simulation, and finally compare the results and accuracy with that of a detailed time-based simulation. Their work shows that the fast computational time of the event-based models compensates the loss of accuracy of the model when comparing it to a time-based simulation, and the authors argue that for determining and solving conflicts at railway junctions the event-based model is suitable and generally a better choice over the more detailed time-based models.

Espinosa-Aranda and García-Ródenas (2012) developed a discrete event-based simulation model with fixed block sections to model the regional railways around Madrid, in Spain. Their objective was to develop a realistic model with the lowest possible associated computational cost. Their simulation tool showed potential to be integrated both into online and offline systems, allowing for the anticipation of conflicts and delays in real-time thanks to simulations only taking a few seconds to run. However, the authors also acknowledge the limitations of their model and the need for a more detailed framework to implement more complex real-time conflict resolution algorithms and strategies.

On a similar note, Xiao-Ming *et al.* (2014) developed a simple discrete event-based model for simulating train movement on a single line. The authors had a greater focus on the energy-saving factor in this case, and conducted an extensive research work covering many case studies to prove the suitability of their event-based model. The model proved to be successful

in simulating the train runs and the interactions between trains in a single-line, with an evident lower number of iterations required when compared to a time-based simulation.

Finally, it is worth mentioning some of the most relevant railway simulation tools developed in university research institutes and that are used not only in academia, but also by specialized consultancies and industry operators. OpenTrack was developed at the Institute for Transport Planning and Systems (IVT) of ETH Zurich, Switzerland, and consists in a microscopic simulation model that functions based on user-defined databases describing available infrastructure, timetables and trains (Nash and Huerlimann, 2004). OpenTrack profits from the advantages of object-oriented programming and combines both discrete and continuous simulation processes.

Previously, RailSys had been developed at the Institute of Transport, Railway Construction and Operation (IVE) of the University of Hannover, Germany (Bendfeldt *et al.*, 2000). RailSys is an infrastructure and timetable optimization environment designed to undertake a wide range of railway planning and management tasks. The program has a strong emphasis on comparing scenarios and determining best alternatives and is also based on a detailed microsimulation model.

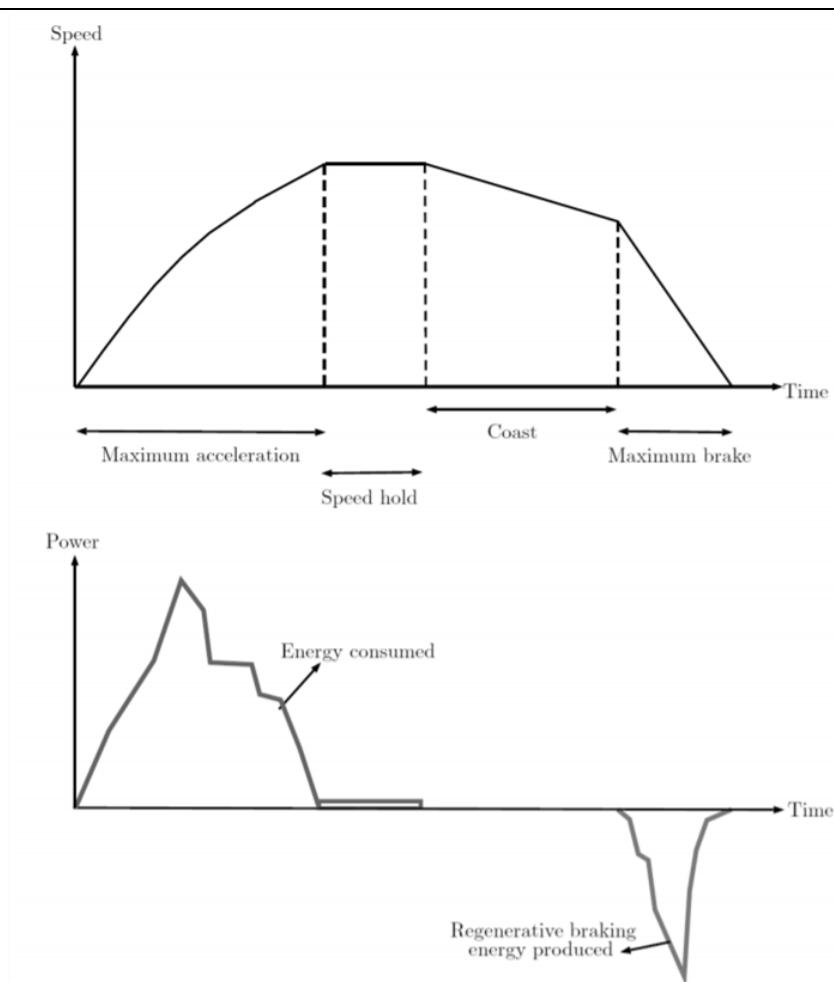
## **2.2 The energy efficient train control problem and other related energy optimization problems**

Extensive research has been conducted regarding the energy efficient design and management of railway networks. This covers from the optimization of individual train runs to the minimization of the energy consumption of railway networks as a whole. Most of the attention has been dedicated to the minimization of the total energy consumption of individual train runs, while meeting timetable and speed limit constraints. This is the well-known optimal train control problem (Albrecht *et al.*, 2016).

This classic problem consists in determining the most energy-efficient trajectory (i.e., speed profile) between two stations such that the overall energy consumption of the train is minimized, subject to a maximum allowable speed for the different track sections, subject to timetable requirements and subject to the different characteristics of the train (e.g., traction power) and railway track (e.g., slope). Typically, the solution to the optimal train control

problem consists in a series of *switching points* where the train changes driving mode. That is, between two stations a train will typically have an initial phase of maximum acceleration until the maximum allowable speed is reached. This is followed by a phase at which this speed is maintained (requiring traction power). Afterwards, the train coasts slowly decreasing its speed, until a final phase of maximum brake is reached (Figure 1). Obviously, this scheme can vary in the case of a variable maximum speed between two stations or based on the slope of the railway track.

Figure 1: Typical speed profile and associated energy consumption



Source: Gupta *et al.* (2016)

The optimal train control problem can be solved formally using optimal control theory and Pontryagin's maximum principle (Albrecht *et al.*, 2016). However, it is most common to

solve the problem numerically or by means of dynamics programming, which has proven to be a very efficient way to deal with the problem (Ko *et al.*, 2004).

The problem of minimizing the net energy consumption requires further considerations when the minimization spans a full railway network instead of individual train runs. Not only must the interactions between trains and other networks effects be taken into consideration, but also other aspects regarding the power supply and energy system of the railway network must be considered. That is, energy efficiency can be conceived from different angles in railway systems.

When aiming to minimize the energy consumption of a railway network, it is very common to tackle the individual train runs' optimization problem together with a timetable optimization. This integrated approach was followed by Zhou *et al.* (2018), where the authors managed to significantly reduce the net energy consumption of a metro system by overlapping motoring and braking sequences of different trains. A similar approach consists in the optimization of train running times by finding running times between stations that minimize the total energy consumption in the network (Montrone *et al.*, 2016). Particularly interesting is the work by Gupta *et al.* (2016), who integrate two optimization models to first obtain the optimal running time of trains to then establish suitable train pairs to maximize the transfer of regenerative braking energy. Regenerative energy braking is generated by trains during the braking phase and can be ideally used to compensate the high energy consumption of other trains during the same instance of time if trains are synchronized accordingly. The work by Gupta *et al.* (2016) shows promising results, since the proposed mathematical formulation of the problem is more tractable than that suggested by other authors.

Due to the mathematical intractability of most approaches, it also common for authors to rely on simulation approaches when dealing with energy-efficiency optimization problems. That is the case in the work by Yang *et al.* (2012), where different simulation approaches were employed to compute the energy consumption and circulation time of trains, in a paper where the authors explored the potential of coasting control strategies to reduce energy consumption in a complex railway network. Their work showed the potential of using detailed simulations to model complex railway networks, since they allow for a realistic representation of the

network and train interactions which is in most cases intractable with a formal mathematical formulation.

Another important aspect emphasized in Gupta *et al.* (2016) is the importance of the electrical substations, and how the considered railway network has to be split into different parts with a unique power supply when performing the different optimization regarding the energy efficiency of the network. Bomhauer-Beins (2019) also discusses how to tackle the electrical substations energy balance problem, and how this can be done either by speed profile optimization, either by timetable optimization or by integrating both approaches together.

Related to this problem is the aim to avoid or at least reduce the power peaks which occur due to different trains running simultaneously in a railway network. This constitutes a different optimization problem regarding the energy-efficient operation of railway networks, since it does not deal with the overall energy consumption in a network but deals with the power demand at every instant in time, trying to avoid sudden surges in demand which could compromise the power supply of the railway network. The problem has drawn much attention recently and tackling it constitutes the basis of this thesis.

## **2.3 Approaches and formulations for the reduction of power peaks in railway networks**

Different authors have proposed a variety of mitigating strategies to reduce or avoid excessive power peaks in railway networks. A review of such approaches is presented hereunder, with a differentiation between real-time scheduling approaches, timetabling approaches and other recent advances in power systems and smart grids.

### **2.3.1 Real-time scheduling approaches**

Online train control approaches mainly consist in determining convenient departure time of trains at stations, by extending their dwell time in order to prevent excessive power peaks such that several trains do not depart stations simultaneously. Although many timetables are already strategically designed as to avoid excessive power peaks in a given railway network (see subsection 2.3.2), delays and disturbances are generally unavoidable and real-time rescheduling is required to avoid putting too much pressure to the power grid.

Yang *et al.* (2019) formulate this as a decision problem where the departure time of the trains at each station must be determined, meaning that for each time instant trains are kept dwelling or are allowed to depart. Consequently, the formulated optimization problem consists in a binary integer program where the objective function balances the minimization of the overall incurred delays with the maximization of energy utilization as long as the power demand remains below a given threshold. The approach proved to be efficient in dealing with power peaks, although it was necessary to include a penalization term for delaying too many trains to avoid the solver being too prone to delay trains and generate equivalent power peaks in futures time instances, just shifting the peaks in time.

In contrast, Albrecht (2010) opted for a train running time control approach instead of dwell time control. The author argues that running time control offers clear benefits when comparing it to dwell time control: on the one hand, the operational difficulties of extending dwell time and the risk of incurring in further delays in the case of late passengers; on the other hand, the additional dwell time could have been more efficiently used to extend the running time of the trains by increasing the duration of the coasting phases, leading to greater energy savings. The approach is promising, since the same effect of delaying the departure time of trains can be achieved by extending the coasting phase before arriving to the station, leading to a further benefit other than the avoidance of the power peaks thanks to the energy savings incurred during the longer coasting phase.

Khayyam *et al.* (2018) suggest a so-called *minute-ahead optimization* consisting in limiting the traction power of different train compositions, based on a previous *day-ahead optimization* where the problematic power peaks were initially identified.

A different perspective of the problem is included in Gu *et al.* (2013), where the authors analyze the power demand peak problem in the particular case of a moving block signaling system. The authors suggest two different mitigating strategies to avoid excessive power peaks: firstly, they suggest a way to avoid the formation of a long queue of trains which would lead to a power peak when they simultaneously accelerate by employing the travel time reserves at the stations and staggering the maximum acceleration phases of the different trains; secondly, for the case where time reserves are not available, the density of the queue is reduced and therefore, the power demand is also decreased.

### 2.3.2 Offline timetabling approaches

In most cases, railway timetables are already optimized to avoid the synchronous acceleration of trains and therefore, avoid unacceptable power peaks in the concerned power supply area. Nonetheless, models have been suggested for timetable adaptation to ensure the avoidance of power peaks. Bärmann *et al.* (2017) suggested a mixed-integer programming model which was tested to make slight adaptations to timetables from the Deutsche Bahn in Germany. The objective was to balance the overall power demand of the trains and increase the stability of the power system, minimizing fluctuations. The model proved efficient in solving the instances with excessive power demand with relatively contained modifications to the original timetable, although this was only tested for relatively small instances.

In a later publication (Bärmann *et al.* 2021), the authors extended their model to larger instances, even reaching a countrywide scale. The authors relied on decomposition approaches and schemes to allow for the computation of efficient solutions in very short time. This time, the objective function allowed for variations based on whether the optimization was to be performed from the perspective of the operating company or the infrastructure manager. The results are very promising, showing great potential for reducing maximum average peak power consumption by shifting departure times of the trains at the different station of network.

However, as already discussed, offline timetabling approaches suffer from the impunctuality issue. Very detailed planning can prove to be insufficient to avoid power peaks in the case of slight delays or disruptions in the network, meaning that it is generally necessary to have a real-time scheduling strategy to reduce the power peaks and therefore keep the power demand below an acceptable threshold. Alternatively, the robustness of the timetabling algorithms and techniques should be guaranteed (Bärmann *et al.*, 2017).

### 2.3.3 State of the art power systems and smart grids

The reduction of power peaks can also be achieved through the implementation of modern power systems allowing for the storage of the regenerative braking energy of trains. This branch of research is complementary to the purely transportation engineering perspective discussed in the previous subsections. Although this work will not focus on this branch of

research, it is worthwhile to include a brief overview of the recent trends of research in this field, since the potential to increase the energy-efficiency of railway systems through the implementation of energy storage systems and smart grids is huge.

For instance, in their paper, Jung *et al.* (2013) discuss ways to utilize regenerative braking energy by integrating different electrically separated railway systems, leading to a reduction of the overall peak power demand as well as optimizing the balances at the individual substations.

Next-generation smart grids consist in the integration of information technologies into the electrical systems to improve its controllability (de la Fuente *et al.*, 2014), allowing for better energy management and control of the power supply and demand of the system. Consequently, smart grids can enable control measures to reduce power peaks, as suggested in the cited publication by de la Fuente *et al.* (2014), by means of introducing capacity limitations in the different electrical grids which conform the railway network. Pankovits *et al.* (2014) implement a fuzzy optimization scheme by favouring local renewable energy consumption and by coordinating the storage of regenerative braking energy in the substations.

An alternative approach to that of storing energy in the substations of the railway network is to equip the trains with onboard energy storage devices. This way, trains can use the stored energy during the phases of maximum acceleration and when their power demand is highest. Steiner *et al.* (2007) confirm the massive energy saving potentials of equipping metro trains with supercapacitors for energy storage, with savings of around 30% of overall traction energy used and a dramatic reduction of the power peak demand. Ciccarelli *et al.* (2012) further investigated the use of supercapacitors in rapid transit systems and confirmed the saving potentials by integrating control strategies for the supercapacitors with motor drive control. Alternatively, Lee *et al.* (2013) suggested the use of superconducting flywheel energy storage systems, again intending to make a better use of the regenerative braking energy produced by train while braking. The results and power peak reduction potential are similar to those argued by Steiner *et al.* (2007). Additionally, the authors present promising figures regarding the economic benefits of such next-generation power storage systems.

## 2.4 Research gap and contribution of this thesis

After an exhaustive study of the available literature and current research trends regarding the reduction of power peaks in railway networks, several research gaps are identified. This study aims to contribute to the field by complementing the available research in a variety of ways.

Firstly, there is very limited research regarding the effect of delays on the magnitude of the peak power demand in a railway network. Although most authors do recognize that delays can contribute to sudden changes in the power demand, and that offline timetabling optimization can become pointless in cases with severe disturbances, no literature has been found covering the actual quantification of power peaks based on the stochastic effects generated in the railway network based on random departure delays of trains at the stations.

Additionally, most of the optimization studies aiming to reduce or avoid power peaks rely on complex mathematical formulations, which end up being *NP*-hard or intractable in most of the cases. Simplifications concerning the infrastructure and the interactions between trains are normally required, thereby losing part of the accuracy and not being able to properly capture the inherent network effects of a complex railway model. Consequently, an optimization based on a detailed simulation model is to be conducted, conserving all the details that characterize the modelled railway network and guaranteeing a realistic representation of the interaction between trains.

Finally, there is very limited evidence of studies suggesting the implementation of power limitation strategies to prevent trains from consuming excessive energy in cases where a high power peak might be generated. Moreover, combining power limitation strategies with the more frequently used departure time shifting (increasing dwell times of trains at the stations) is a further contribution of this work.

### 3 Development of a simulation tool for the quantification of the power consumption of trains in a railway network

#### 3.1 Case study: The canton of Ticino in Switzerland

A specific study area has been selected for this work. The area includes two main railway lines in the Canton of Ticino in southern Switzerland. The selected area is suitable for this work since it combines a very busy line with a relatively unbusy one, and has well delimited power supply. Additionally, there are railway junctions in the network and a variety of trains with different stopping patterns (from regional to long-distance), meaning that the simulation will be sufficiently detailed and enthralling without being overly complex and requiring a huge computational power.

Although this specific case study has been selected, the simulation has been developed ensuring its generalizability, meaning that with simple adaptations it can be easily employed to model other scenarios and networks.

##### 3.1.1 Railway lines considered

Figure 2 depicts the railway network in the Canton of Ticino, including all connections to the rest of Switzerland through the Gotthard tunnel and international connections with Italy. The railway lines considered are those around Cadenazzo, including the lines starting in Locarno and Luino. Table 1 and Table 2 include a summary with the lines that have been considered for this case study. Figure 4 in section 3.2 will present the track configuration covering the considered lines.

Table 1: Train lines departing from Locarno

Line	Destination	Stops	Frequency (per hour)	Trains in the simulation
S 20	Castione-Arbedo	All	2	11, 12, 13
RE 80	Chiasso/Milano	All until S. Antonino	2	41, 42, 43
IR 26/46	Basel/Zurich	Tenero, Cadenazzo, Giubiasco, Bellinzona, Castione-Arbedo	1	31

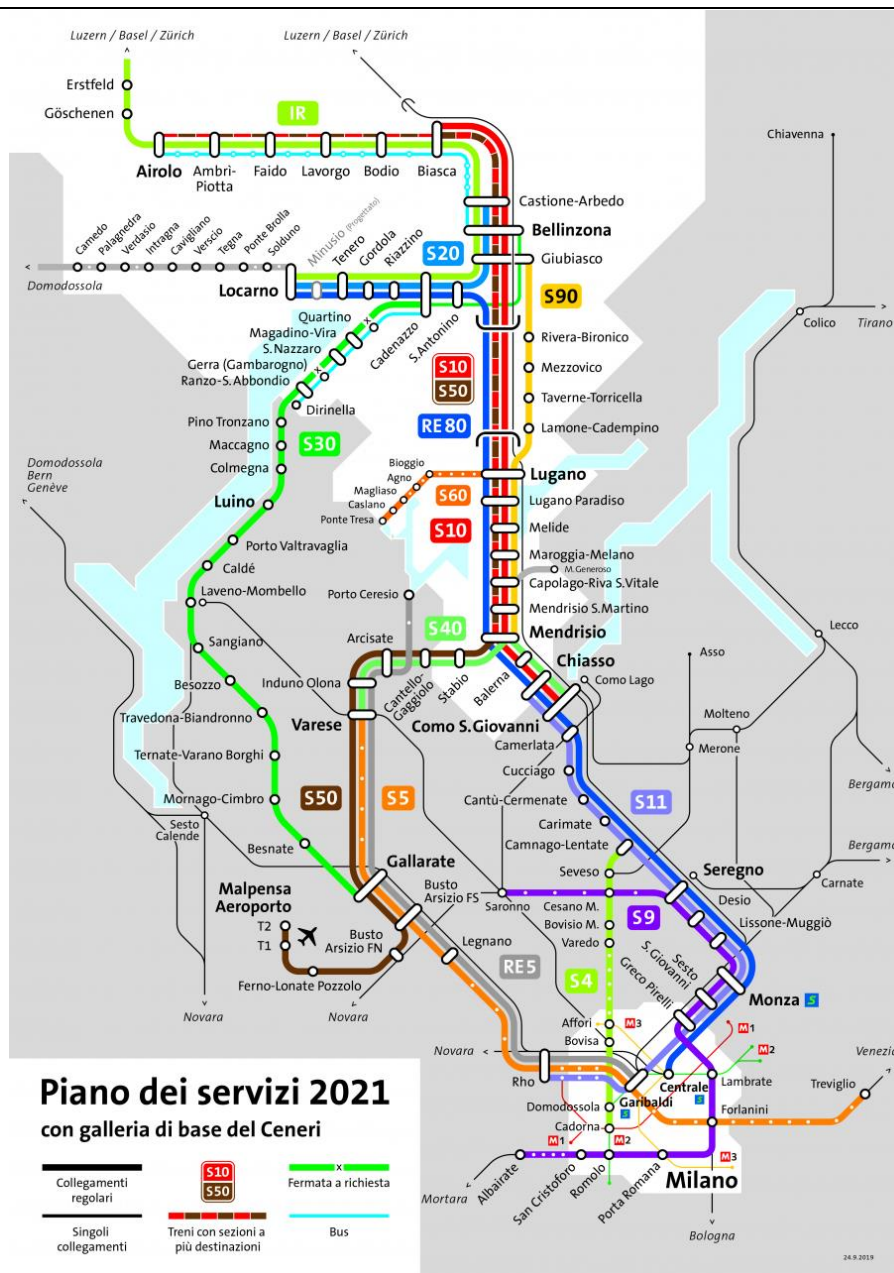
Source: SBB

Table 2: Train lines departing from Luino

Line	Destination	Stops	Frequency (per hour)	Trains in the simulation
S 30	Cadenazzo	All	1	21, 22

Source: SBB

Figure 2: Railway lines in the Canton of Ticino, updated 2021 after the opening of the Ceneri base tunnel



Source: www.tio.ch

It must be noted that line RE 80 entered in service in early spring 2021, following the opening of the Ceneri base tunnel. Additionally, line S 20 was reconfigured and now terminates at Castione-Arbedo, whereas it went all the way to Biasca before.

The Inter Regio trains (IR) provide some heterogeneity in the railway traffic, since they are express services that do not stop in all the stations. The timetables of all lines were adapted after the new infrastructure development and the updated timetables have been used in this study.

### 3.1.2 Rolling stock

For simplification purposes, two different train configurations have been used in the simulation (Figure 3). Their technical details are shown in Table 3.

Table 3: Rolling stock considered in the simulation

Train type/Locomotive	Power	Traction force	Mass	Lines used
SBB Re 460	6100 kW	300 kN	354 t	S 20, RE 80, S 30
TiLo Flirt RABe 524	2600 kW	200 kN	131 t	IR 26/46

Source: SBB

Figure 3: SBB Re 460 locomotive (left) and TiLo Flirt RABe 524 regional train (right)



Source: Wikipedia (left) and Stadler (right)

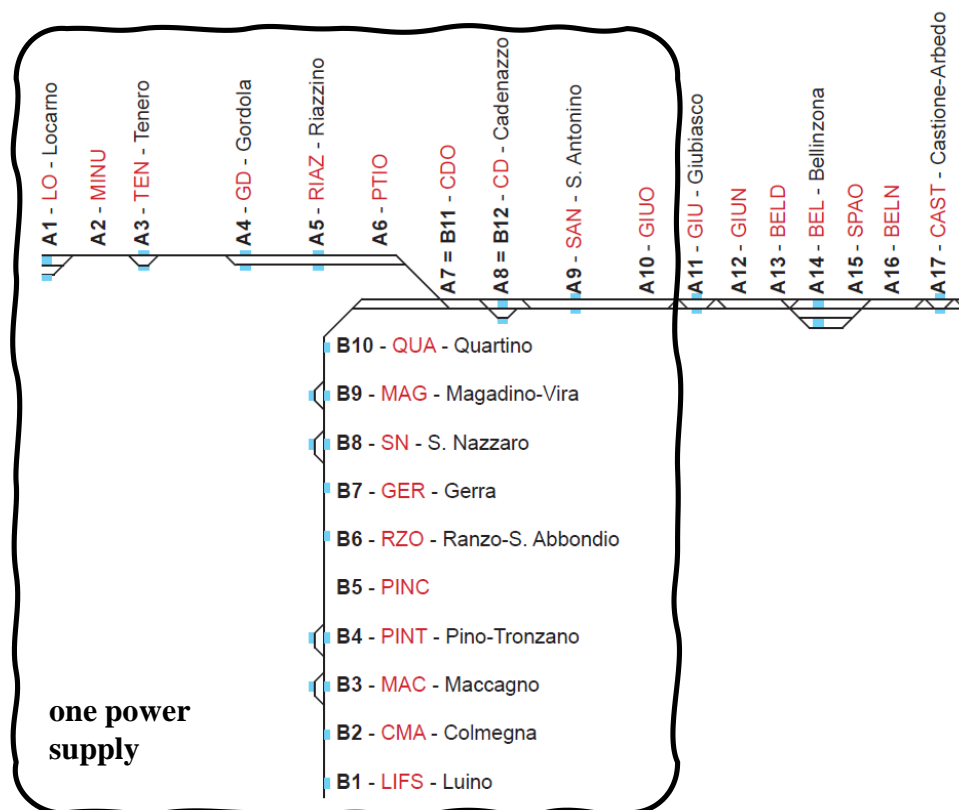
## 3.2 Simulation inputs

### 3.2.1 Infrastructure

Figure 4 shows the track layout of the considered railway network. The line going from Locarno to Castione-Arbedo is designated as line A and the line going from Luino to Cadenazzo is designated as line B. The block sections are also defined, corresponding to the existing signaling locations of the network.

Additionally, the power supply area of interest is delimited in the figure. It is the purpose of the simulation to quantify the power demand of trains when they are inside this area. For this reason, Inter City (IC) trains going from Bellinzona towards Lugano are not included in the simulation.

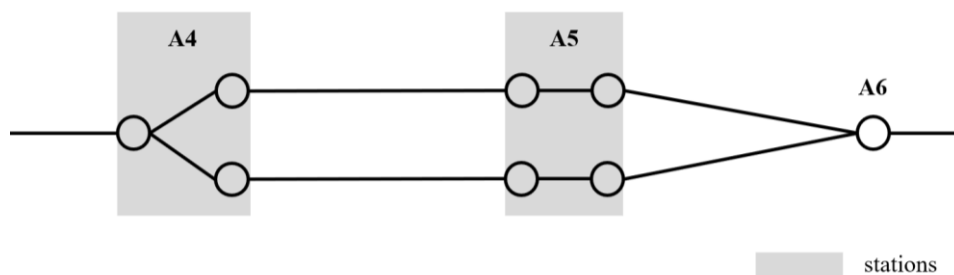
Figure 4: Considered network with block sections and delimitation of the power supply area



Source: own elaboration from SBB data

The network is modelled by means of a graph, consisting of nodes and edges. For this purpose, individual block sections are represented by one edge, as well as stations. The illustrative example in Figure 5 shows how the track sections between A4 and A6 are modelled. Obviously, information regarding single and double-track section are conserved in the simulation.

Figure 5: Graph representation of the railway network



Source: own elaboration

Input files describing the infrastructure initially assume double-track sections throughout the entire network, meaning that individual track sections must be deactivated in those cases with single-track sections. From the list of stops of each line, the simulation produces an ordered sequence of all the links which the trains of that particular line must cover.

### 3.2.2 Timetable information

The timetable information corresponds to the official departure times of trains at the stations (with a 1-minute resolution), as published by SSB in spring 2021 after the opening of the Ceneri base tunnel. A particular timetable is generated for each of the trains running in each line, as specified in the last column of Table 1 and Table 2.

A default value for the dwell time at the stations is also given. For this work, a value of 40 seconds is used for all trains and all stops.

### 3.2.3 Train trajectories and associated power consumption

Specific trajectories for each train type corresponding to each of the sections of the network (Figure 4) are calculated before-hand and used as inputs in the simulation. This is performed

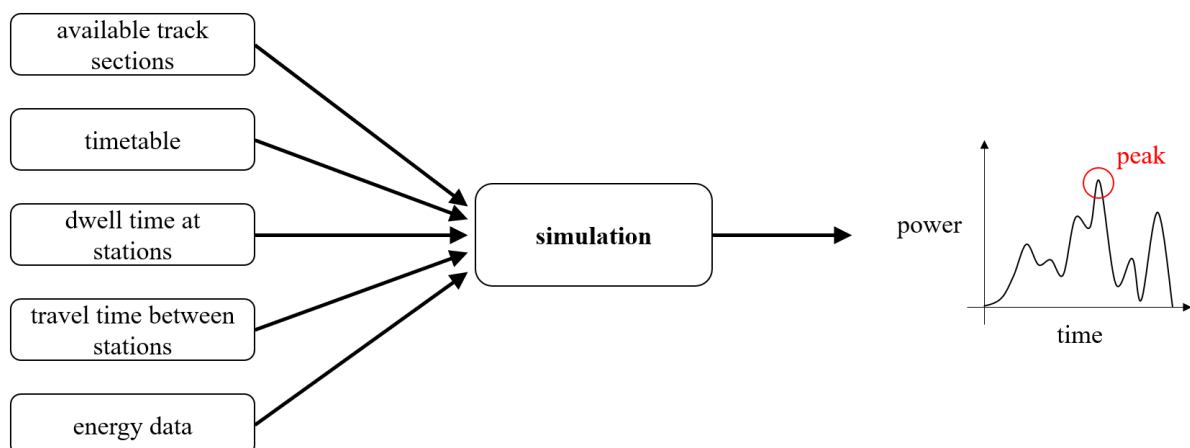
using a specific tool developed by PhD student Michael Nold at the Institute for Transport Planning and Systems (IVT) of ETH Zurich. The tool is capable of computing very detailed power consumption profiles based on rolling stock configurations and infrastructure definition (slope, radii of curves, maximum allowable speed, etc.). The resulting tables containing time-speed-distance-power relationships are all prepared as inputs for the simulation. It must be noted that the tool computes trajectories with the highest possible acceleration and deceleration, meaning that the resulting power consumption profiles correspond to the worst case scenarios, i.e., those with the greatest energy consumption and no coasting phase.

The power consumption profiles are computed for each of the four possible driving schemes (refer to section 3.3), and the total driving time of each section is then associated to the list of links to be covered by each line (links corresponding to stations have a null travel time).

### 3.3 The simulation

The purpose of the simulation is to use the inputs described in section 3.2 to model the movement and interactions of the trains following the timetable in order to quantify the power peaks during a given simulation horizon (Figure 6). For this work, the simulation horizon considered will be of 2 hours, which is suitable for the analysis and propagation of delays. When following the normal timetable cycles are of 60 minutes, as will be verified later.

Figure 6: Schematic summary of the simulation inputs and outputs



Source: own elaboration

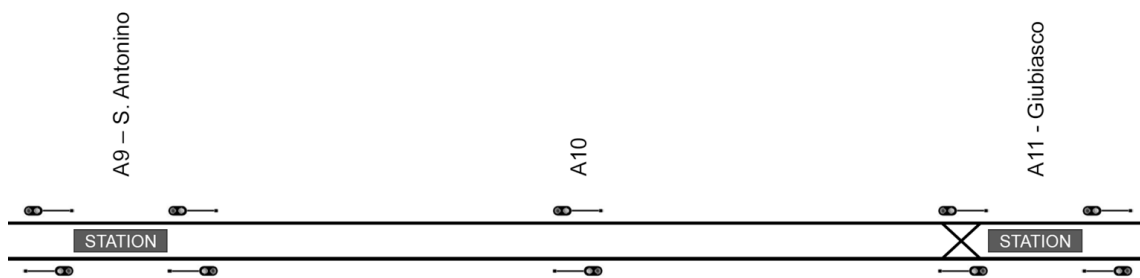
---

The proposed simulation follows the theory of discrete event-based simulations. Events are defined as trains moving from one link to the next, i.e., advancing section. The simulation is solely updated after an event occurs, although at every time instance it is checked whether an event can happen or not. That is, following a predetermined time step (typically either 1 second or 5 seconds), the time of the simulation is updated, and it is checked whether an event should happen in order to update the corresponding attributes of the simulation. Although a time step of 5 seconds favours the reduction of the computational cost of the simulation, some inconsistencies can occur due to the rounding of times, so a time step of 1 second results in a better choice when the outputs shall be obtained with maximal accuracy.

Independently of the time step, the energy data is provided in a 1-second resolution, meaning that the output in terms of power demand always conserves this 1-second resolution.

The signaling system considered corresponds to that of a fixed-block system. For the stations, signals are considered to be before and after the platform, separated by a distance of 300 meters (Figure 7). This way, trains can stop before the station if the track is occupied by another train, and then advance to the second signal once the first train leaves the station. Special power consumption profiles are included in the simulation for this specific movement.

Figure 7: Detail of the block sections and signaling at the stations

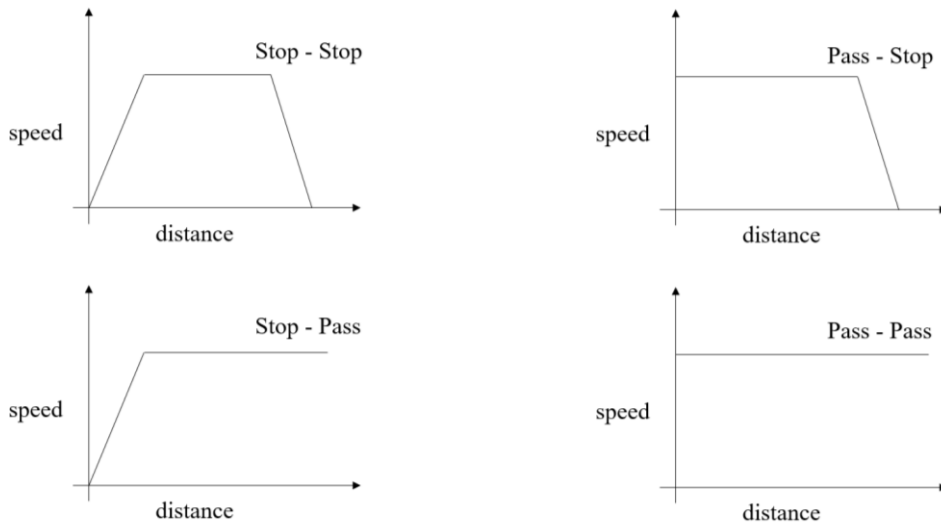


Source: own elaboration

---

As a consequence of the signaling system employed, different driving schemes are defined for each of the sections. These correspond to the train being stationery or moving at the initial and final signal of the section, meaning that there are four possible driving schemes as shown in Figure 8. Evidently, the simulation ensures that only compatible driving schemes are concatenated.

Figure 8: Possible driving schemes between two signals



Note: the speed profiles are simplified for illustrative purposes. Source: own elaboration

There are fundamentally two different dynamic arrays in the simulation, which are updated after each event. Firstly, there is an array for each line, including the currently occupied link, the driving scheme and the time of the next event for each of the trains of the line. Secondly, there is a list with of all the links of the network indicating whether they are currently occupied or not. In case a link is occupied, the train occupying it is identified. This occupancy table also indicates those links which are currently not occupied but are *reserved* for a particular train since they will be unavoidably occupied in the future by that train. There are typically two situations where a track section must be reserved:

- When the driving scheme involves the train not stopping at the next signal, the subsequent link must be reserved.
- When the train enters a single-track section, all subsequent links must be reserved until the following double-track section.

The time of an event is defined either as the departure time from a station as computed using (5a and 5b), or as the time at which a train will complete a given section (if the currently occupied link does not correspond to a station).

$$\text{departure time} = \max(\text{arrival time} + \text{dwell time}, \text{timetable departure time}) \quad (5a)$$

$$t_{dep} = \max(t_{arr} + t_{dwell}, T_{timetable}) \quad (5b)$$



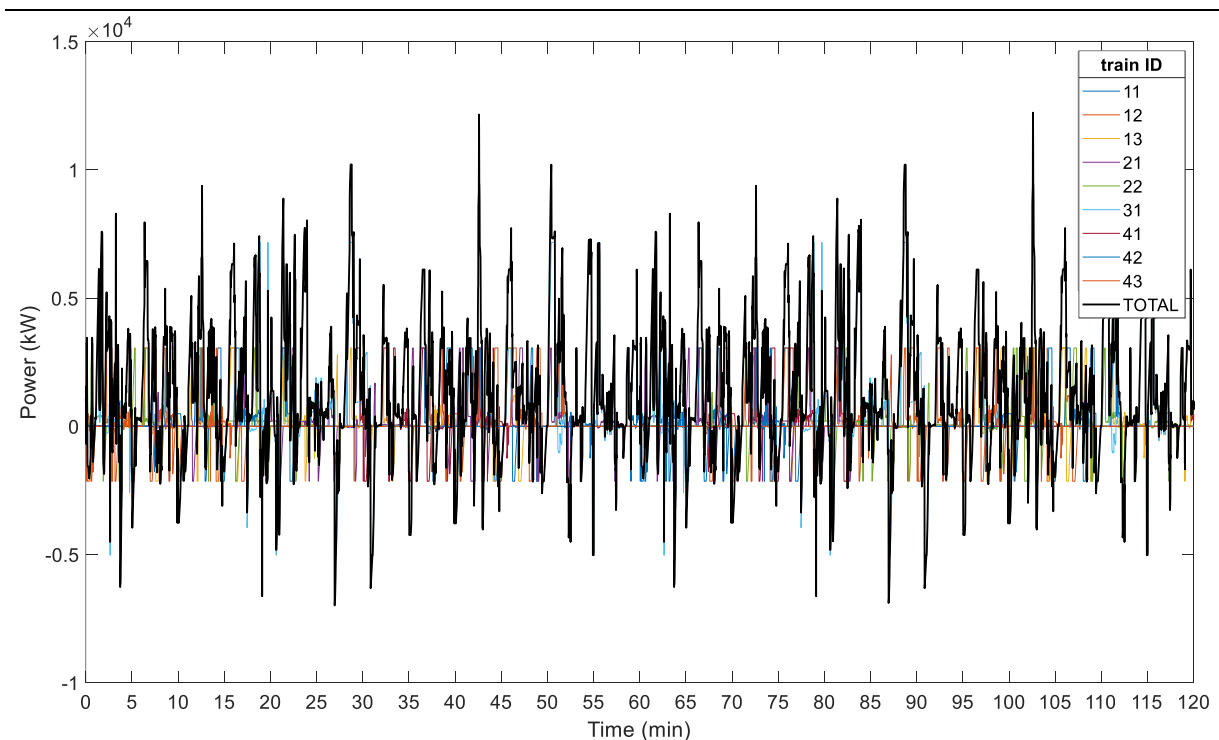
## 3.4 Simulation outputs

### 3.4.1 Power demand profile

The fundamental output of the simulation corresponds to the power demand profile of all trains throughout the simulation horizon. This is shown in Figure 10. The plot includes the contribution of all trains, and only considers energy consumption when trains are inside the power supply area (Figure 4, computed following equation (1)). Minute 0 in the outputs does not actually correspond to the initial instance of the simulation. In fact, at the beginning of the simulation there is a warm-up phase where trains are gradually introduced in the simulation. Only after the warm-up phase is completed, does the *real* simulation spanning two hours begin.

It can be observed how the results are identical from minute 0 to minute 60 and from minute 60 to minute 120. This is due to the fact that the timetables of the considered train lines have all a frequency of at least 1 train/hour. The highest peaks are identified at minutes 42 and 102 of the simulation and correspond to a power demand of 12236 kW (refer to equation (2)).

Figure 10: Power demand profile during the simulation horizon



Source: simulation output

### 3.4.2 Rolling averages and other indicators for power consumption

In order to further analyze the power demand profile depicted in Figure 10, it is convenient to include power consumption values corresponding to the 90<sup>th</sup>, 75<sup>th</sup> and 50<sup>th</sup> (median) power demand percentiles. Additionally, the power demand profile can be smoothed by computing the profile with a 5 or 10-second moving average. Table 4 summarizes these results.

Table 4: Power peak and other indicators using rolling averages

Indicator	1-second	5-second average	10-second average
Power peak	12236 kW	10412 kW	10156 kW
90 <sup>th</sup> perc. power	5099 kW	4741 kW	4459 kW
75 <sup>th</sup> perc. power	3054 kW	2833 kW	2750 kW
50 <sup>th</sup> perc. power	896 kW	921 kW	987 kW

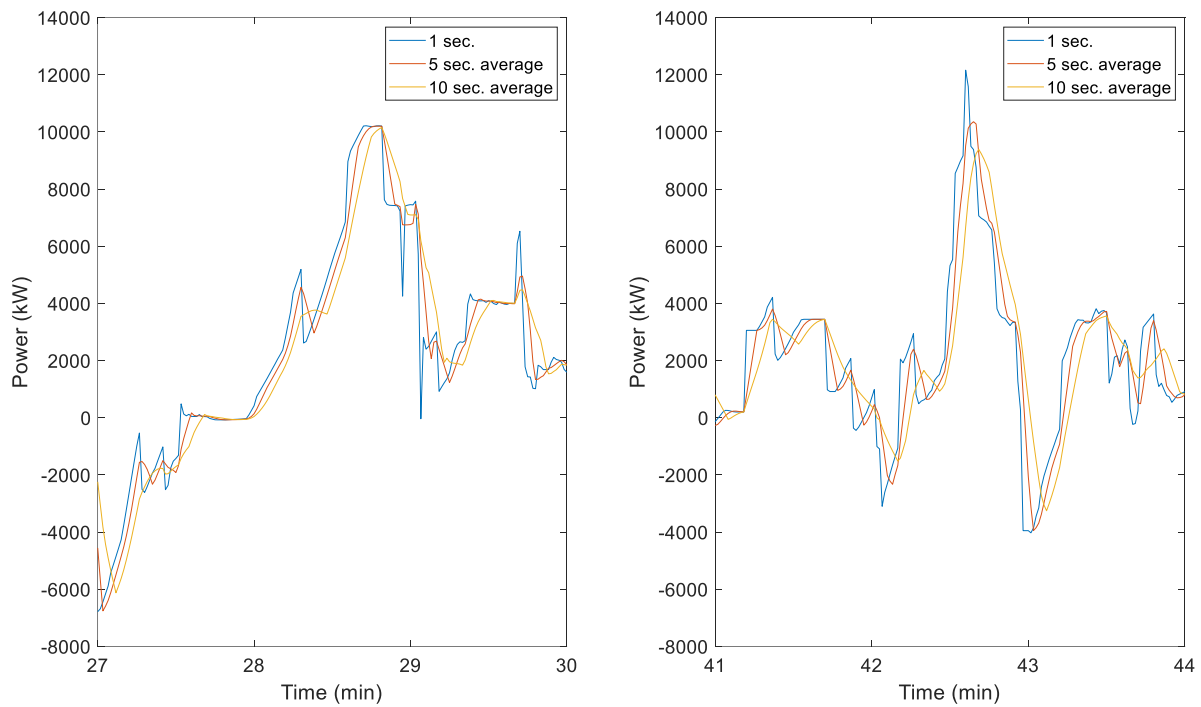
Source: simulation output

It is noticeable how the 90<sup>th</sup> percentile power consumption values are already more than 50% lower than the power peaks, confirming that the power peaks are a punctual phenomenon in most of the cases.

Of particular interest is the study of the peaks using different rolling averages. In Figure 11, the power demand profiles with different rolling averages around the peaks can be compared. On the left plot, it can be seen how the magnitude of the peak is equivalent for all three profiles since the peak power consumption is sustained for a few seconds.

However, on the right plot, a peak where its magnitude clearly differs when using different rolling averages is identified. This is because the peak consumption corresponds to a very punctual instance and is not sustained in time. Consequently, the rolling average smoothen the profile and lower the magnitude of the peak. The 10-second rolling average, nonetheless, provides excessive smoothing as can be appreciated in the figure. Most of the minor peaks are completely eliminated when using the 10-second average, and this is regarded as losing some of the meaningfulness of the results. Consequently, the 5-second rolling average is selected as the preferred indicator, capable of neglecting the very punctual effects while providing a reasonable smoothness level to the power profile.

Figure 11: Power peaks using different rolling averages



Source: simulation output

### 3.4.3 Delays

The simulation is capable of providing outputs regarding the actual departure delays of trains at the stations. It must be emphasized that train may be unable to depart a station even though indicated by the planned departure time if the following links are occupied by other trains. Delays can be easily computed by comparing the actual departure time of trains from a station with the planned departure time according to the timetable.

It must be noted that already when running the simulation using the normal timetable (without stochastic delays), some trains do depart late from stations. This is due to some inconsistencies regarding the predetermined trajectories of the trains, which were calculated using a specific tool independently from the SBB published timetables.

Simulation outputs and results regarding delays will be presented in Chapter 4.

### 3.4.4 Train trajectories

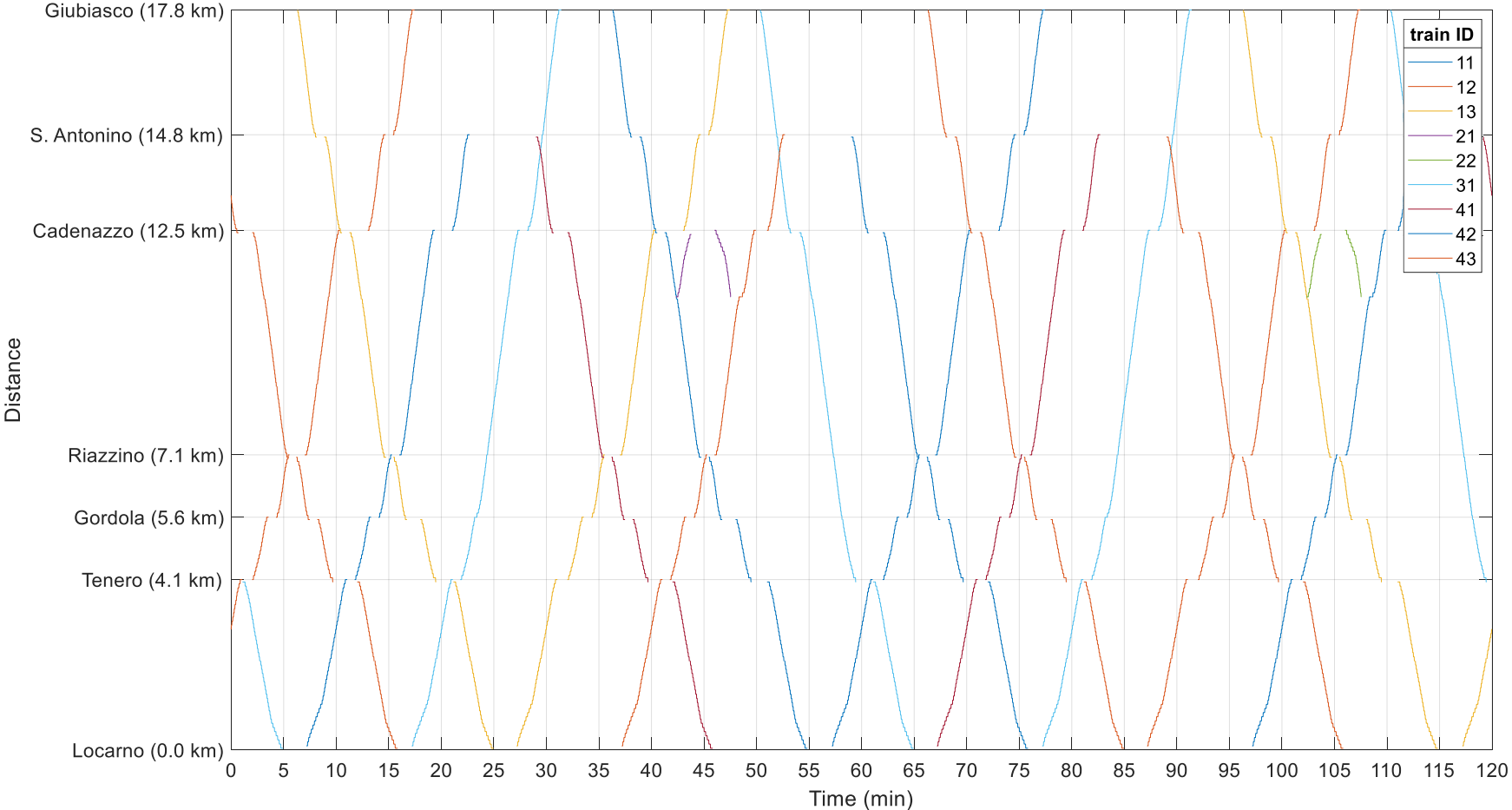
An additional output of the simulation allowing for the visual interpretation of the train movements is presented in Figure 12. The train trajectories during the simulation horizon are included, between the stations of Locarno and Giubiasco. It must be reminded that as presented in Figure 4 the considered power supply covers the area to the east of Giubiasco.

Trains from line S 30 (Luino – Cadenazzo) are also included, when covering the section between Cadenazzo and the CDO signal (Figure 4). Trains from line RE 80 are included until S. Antonino, since they then deviate from the main railway line towards Lugano through the Ceneri base tunnel.

The trajectories depicted in Figure 12 allow for a comprehensive analysis of the train movements and interactions, as well as allow for the verification of the well-functioning of the simulation. Again, it can be observed how the trajectories during the first hour of the simulation are identical to those during the second hour due to the frequencies of the trains being of at least 1 train/hour. Additionally, it can be verified how train 31 (corresponding to the IR train) skips stops as defined by its timetable and stopping pattern. Also, the correct occupancy of single-track sections and the intersection of trains always in double-track section can be confirmed.

It is noticeable how busy the section between Locarno and Gordola is, bearing in mind that the railway line is single-track other than at the stations in this area. The block sections between Locarno and Tenero and between Tenero and Gordola are occupied almost all of the time, due to the fact that three different lines use those tracks and terminate at Locarno, where 3 platforms are available (one used for each line).

Figure 12: Train trajectories during the simulation horizon



Source: simulation output

## 4 Delays, timetable variation and stochastic effects

### 4.1 Delay scenarios considered

Different delay scenarios have been considered in this study, and have therefore been included in the simulation in order to study the effect of impunctuality on the magnitude of the power peaks. Delays are always included in the simulation as departure delays in the stations. Several studies, such as those carried out by Yuan (2006) or Bergström and Krüger (2013), debate between the suitability of different probabilistic delay distributions to adequately model the departure delays of trains. The preferred models include either Weibull (6) or exponential distributions (7).

$$f_X(x) = \lambda\alpha(\lambda x)^{\alpha-1}e^{-(\lambda x)^\alpha} \quad (6)$$

$$f_X(x) = \lambda e^{-\lambda x} \quad (7)$$

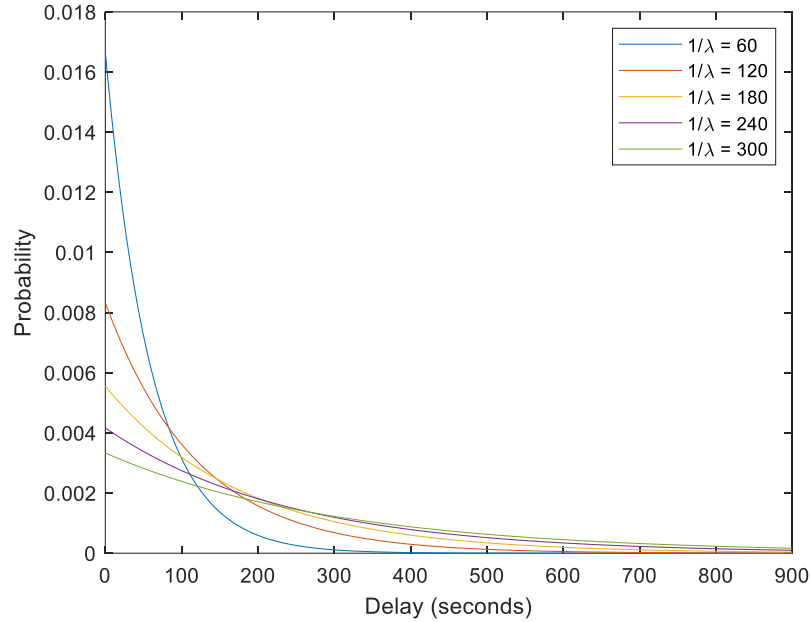
In the case of the Weibull distributions, there is not a clear rule on correctly determining the shape parameter  $\alpha$ . This is done normally by fitting the distribution to the available data, with  $\alpha$  adopting values either above or below 1, depending on the modelled scenario. Consequently, in this work, a value of  $\alpha = 1$  is assumed, meaning that the Weibull distribution simplifies into an exponential distribution, which can be considered as a specific case of the Weibull distribution when the shape parameter is set to 1.

The interpretation of  $\lambda$ , in contrast, is easier since its inverse value corresponds to the expected value when sampling the distribution. The median value, however, is lower than the expectancy (8) due to the higher probability of sampling lower values when using exponential distributions.

$$M_e = \frac{\ln(2)}{\lambda} \quad (8)$$

Figure 13 shows the probability density distributions assuming different values of  $\lambda$ .

Figure 13: Probability density functions of some of the delay distributions used



Source: own elaboration

As indicated previously, delays are sampled from the exponential distributions and included in the simulation as departure delays. This means that the departure time ( $t_{dep}$ ) from a station which had been previously computed using (5a) and (5b), is updated to  $t'_{dep}$  by adding the newly sampled random dwell time ( $t_{random}$ ) as a delay on top of it (9a, 9b):

$$\text{departure time}' = \text{departure time} + \text{random dwell time} \quad (9a)$$

$$t'_{dep} = t_{dep} + t_{random} \quad (9b)$$

$$t_{random} \sim \text{Exp}(\lambda) \quad (10)$$

Different values of  $\lambda$  are used in each of the delay scenarios, to study the sensitivity of the parameter and whether higher expected delays lead to greater changes in the power peaks or not. Three delay scenarios have been considered:

- Delay scenario 1: Delaying all the trains at all the stations.** In this scenario, every time a train stops at a station, the departure time is updated using (9a, 9b) by sampling a random value from the considered delay distribution. For this scenario, a special case is included when sampling delays with an expected value of 2 minutes ( $\lambda=1/120$ ). This case, denoted hereafter as  $\lambda=1/120^*$ , consists in shifting the delay by subtracting

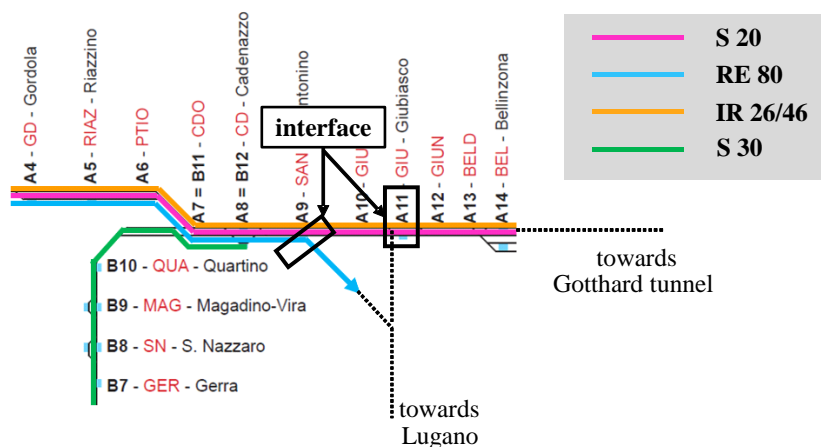
60 seconds after sampling from the distribution (11a, 11b). This way, it is possible to have trains departing slightly ahead of schedule. This special case accounts for the situations in which driver sometimes accelerate and leave the stop a few seconds before the exact departure minute.

$$\text{departure time}' = \text{departure time} + \text{random dwell time} - 60 \text{ sec.} \quad (11a)$$

$$t'_{dep} = t_{dep} + t_{random} - 60 \quad (11b)$$

- **Delay scenario 2: Delaying trains only in the interface.** This scenario considers delays occurring only in the interface, i.e., in the stations where the considered power supply area meets the rest of the railway network (Figure 14). The interface connects the considered network part with the mainline running from the Gotthard tunnel towards Lugano and Italy via Chiasso. This scenario replicates the case where trains are heavily delayed in the mainline, meaning that the delays are included when they enter the considered supply area in the interface.
- **Delay scenario 3: Combination of scenarios 1 and 2.** Delay scenario 3 combines a specific case of each of the two former scenarios. In particular,  $\lambda=1/120^*$  is used for the delays at all the stops other than in the interface, where a greater delay is assumed by using  $\lambda=1/300$ .

Figure 14: Interface between the power supply area and the rest of the railway network



Source: own elaboration

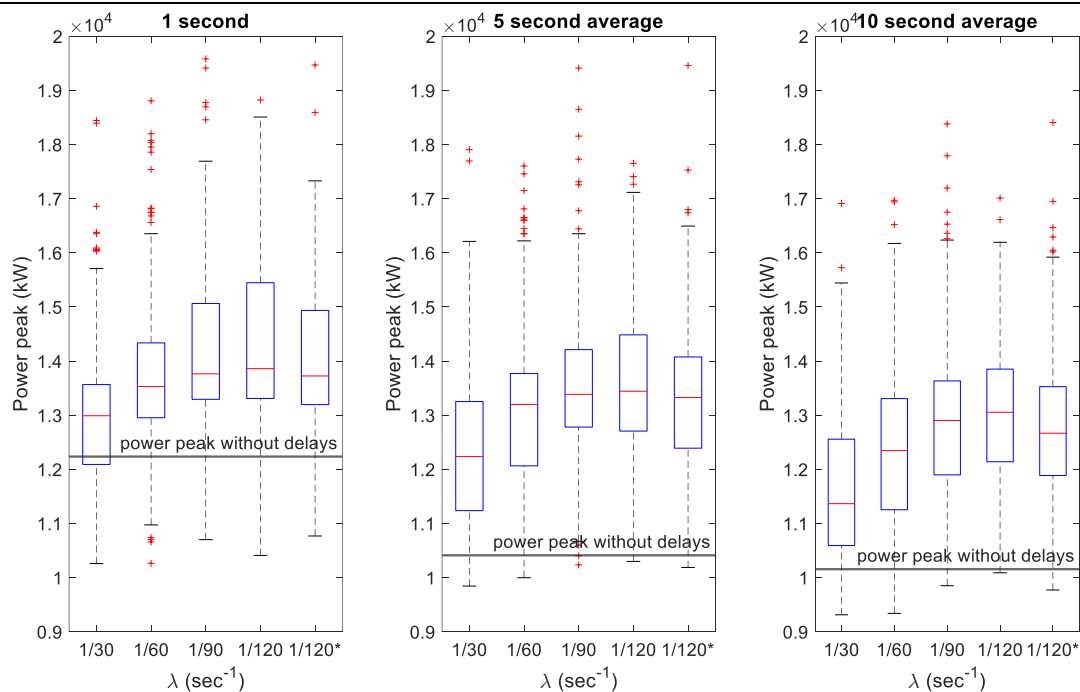
## 4.2 Results and discussion

Due to the stochasticity of the simulations when including the delays, for each of the described scenarios a total of 200 runs of the simulation were conducted. The results presented hereunder reflect the outcome of the 200 simulations that were conducted for the different values of  $\lambda$  in each scenario.

### 4.2.1 Delay scenario 1

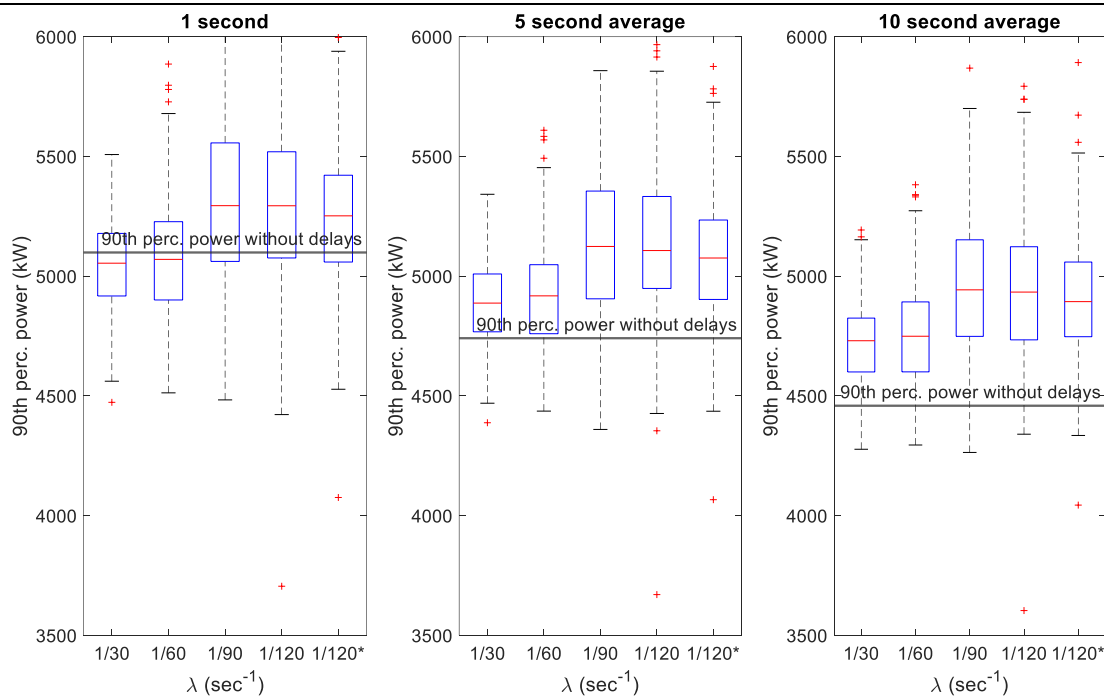
Figures 15 thru 17 present the overall results of the simulations, by showing in the form of boxplots the values for the power peak (Figure 15), 90th percentile power (Figure 16) and 50th percentile power (Figure 17) when sampling delays with different values of  $\lambda$  ranging from  $1/30$  to  $1/120$  seconds<sup>-1</sup>, including also the special case  $1/120^*$ . For each case, results considering a 1-second resolution for the power profile, as well as smoothened cases with a 5 and 10-second rolling average are presented.

Figure 15: Results of delay scenario 1 (power peak)



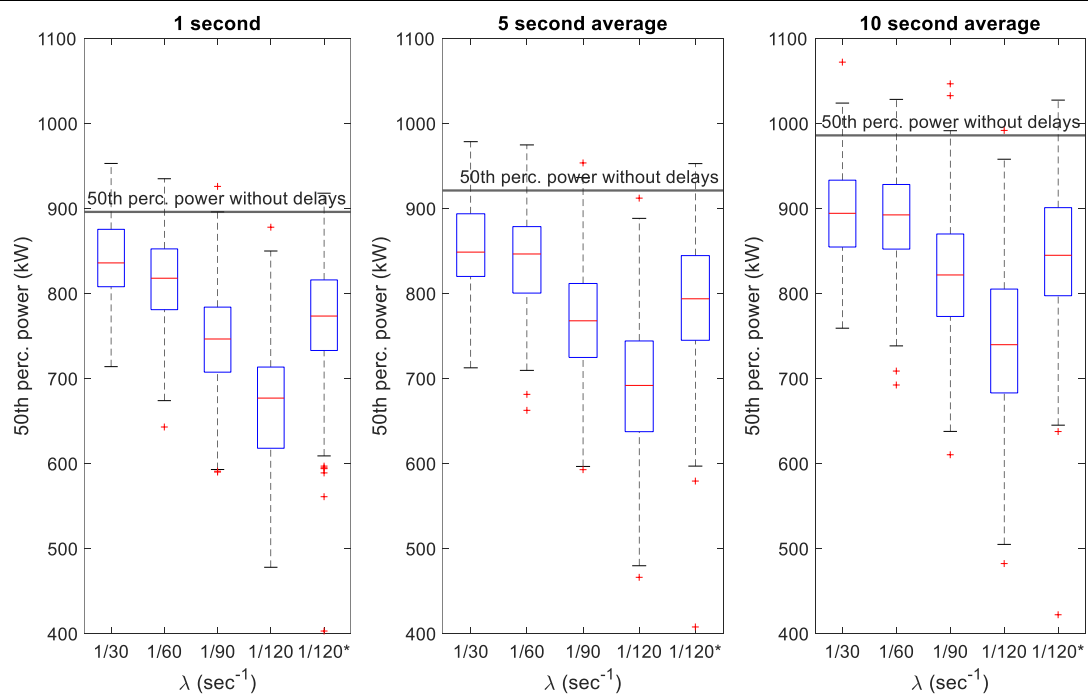
Note: horizontal lines indicate results in the case without delays. Source: own elaboration

Figure 16: Results of delay scenario 1 (90<sup>th</sup> perc. power)



Note: horizontal lines indicate results in the case without delays. Source: own elaboration

Figure 17: Results of delay scenario 1 (50<sup>th</sup> perc. power)



Note: horizontal lines indicate results in the case without delays. Source: own elaboration

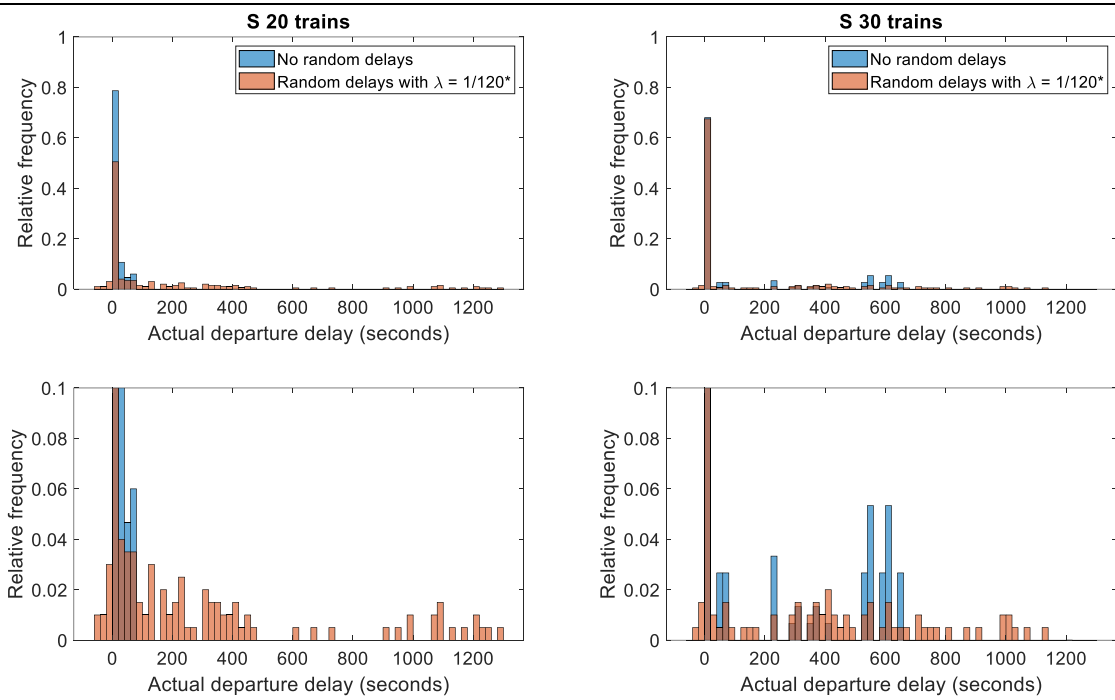
The results shown in Figure 15 immediately confirm that the delays contribute to generate higher peaks in magnitude when comparing them to the base scenario (without delays). The median values of the power peak increase following an increase in the expected delay from 30 to 60 seconds, but then remain constant all the way to a value of 120 seconds of expected delay. It is worthwhile emphasizing how the median value for the power peak remains fairly constant between 13000 and 14000 kW independently of the  $\lambda$  used in the delay distribution. However, the highest upper quartile is detected in the case with the highest expected delay, i.e., 120 seconds. In contrast, most of the extreme points (outliers) take place with an expected delay of 90 seconds, and not 120 seconds. The magnitude of the peaks in these extreme cases are close to 20000 kW even when computing them using a 5-second rolling average, which is almost twice as high as the base scenario.

Overall, the results show the importance of the stochastic effects happening in the network, which are caused by the delayed trains. The simulation is used as a *black box* where many interactions between trains occur, leading to the different power demand patterns. Delays are sometimes propagated, sometimes recovered thanks to sufficient buffer times, etc. The fact that the power peaks sometimes decrease with respect to the base scenario must also be remarked. In this regard, there is greater tendency for this to happen when using lower values of  $\lambda$ .

The values for the 90<sup>th</sup> percentile power also increase in most cases, other than for expected delays of 30 and 60 seconds when computing the values with a 1-second resolution without any smoothing. The variability of the 90<sup>th</sup> percentile value is, as expected, lower than that of the power peak, and remains between 4500 and 5500 in most cases. It is significant to point out the fact that the median power consumption (50<sup>th</sup> percentile) actually decreases when implementing the delays. Most likely, this is caused by the fact that when delaying the trains there is in fact a smaller rate of train moving during a given period, meaning the power demand for this period of time actually decreases, as consequence so does the 50<sup>th</sup> percentile value of the overall power demand. To confirm this, in the most extreme case with expected delays of 120 seconds, the values for the 50<sup>th</sup> percentile power are the lowest with a significance difference with respect to the other cases.

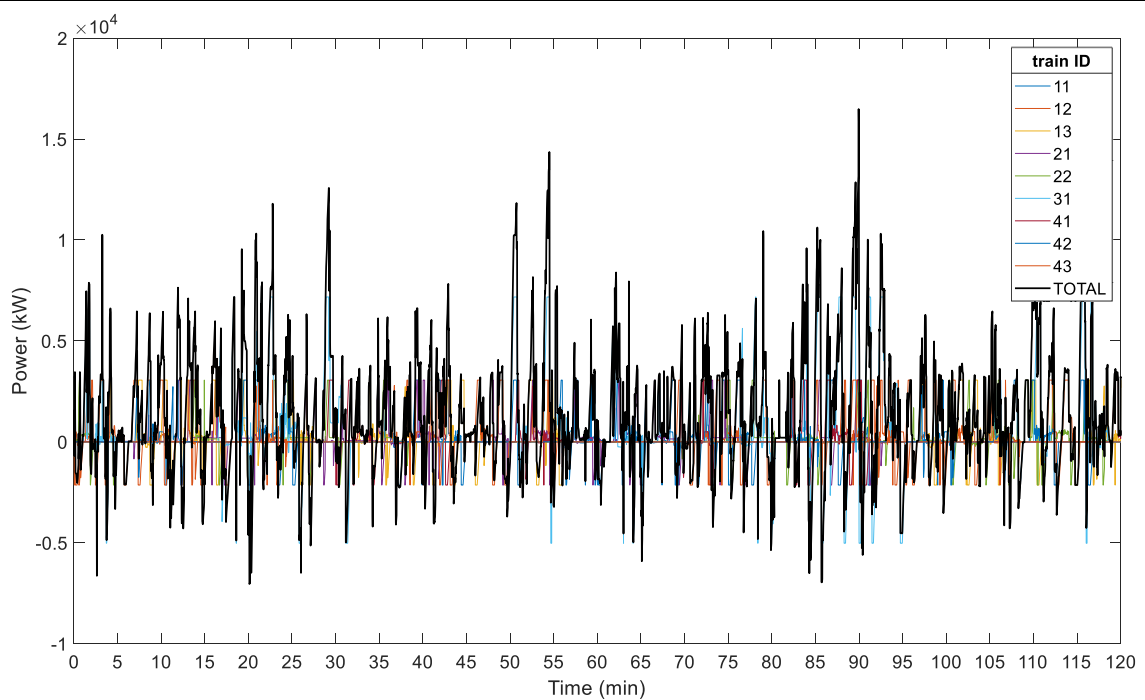
Figures 18 thru 20 correspond to the analysis of a particular simulation run, with  $\lambda = 1/120^*$ .

Figure 18: Distribution of the actual departure delays of train from lines S 20 and S 30



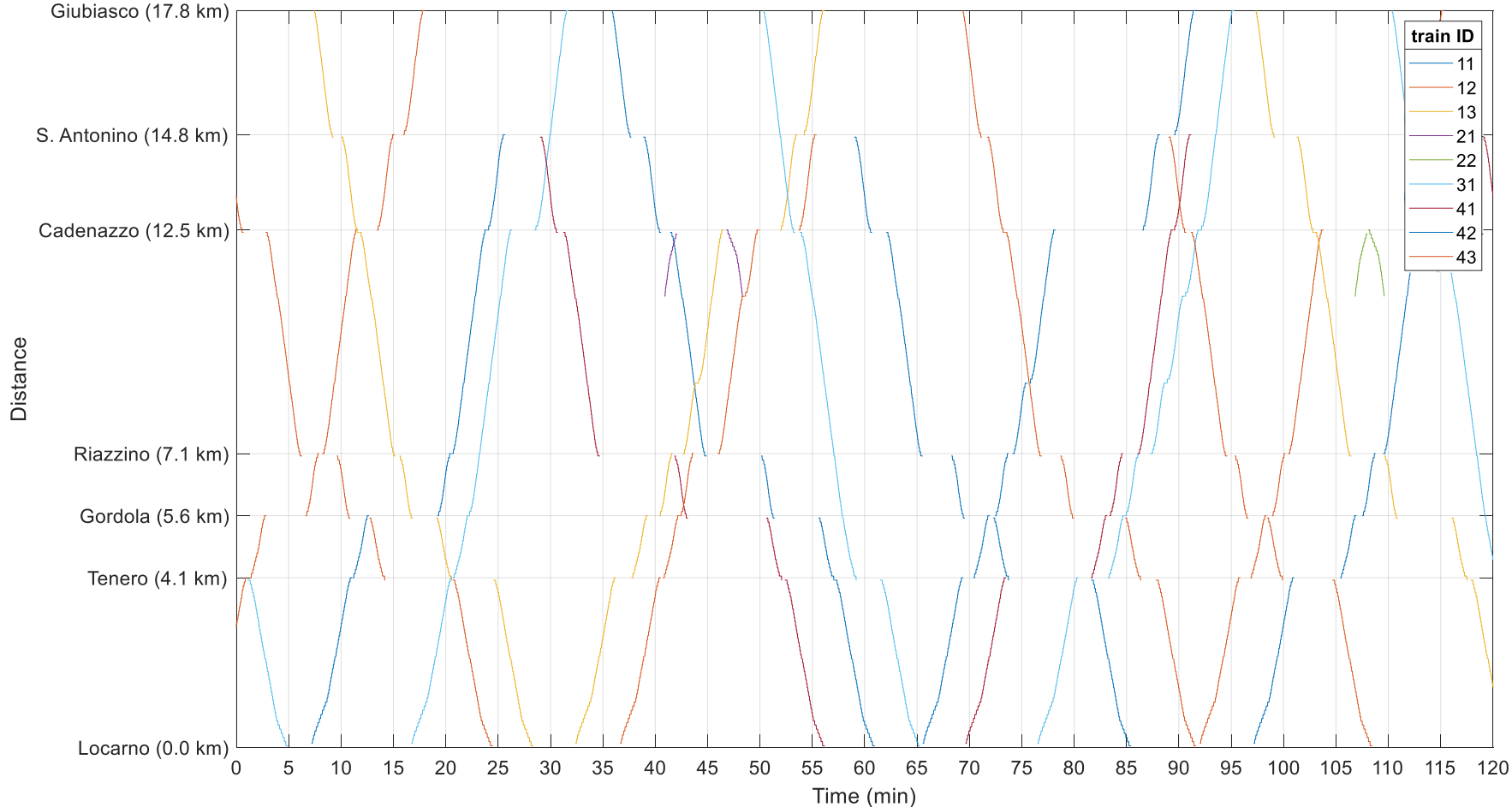
Note: lower figures are a zoom in of the upper figures. Source: own elaboration

Figure 19: Power demand profile during the simulation horizon (delay scenario 1)



Note:  $\lambda=1/120s^{-1}$  and negative shift of 60s considered. Source: simulation output

Figure 20: Train trajectories during the simulation horizon (delay scenario 1)



Note:  $\lambda=1/120s^{-1}$  and negative shift of 60s considered. Source: simulation output

In Figure 18, the actual departure delays at stations of lines S 20 and S 30 in the case of stochastic delays are compared to those corresponding to the base scenario. Actual departure delays are not equivalent to the random delays sampled from the distributions but correspond to the difference between the actual departure time of a train and the departure time according to the timetable (12). It must be noted that the simulation may determine that a train may not be able to depart even though all the random delay time has been consumed if the following link is not available (either it is occupied or *reserved* by another train). For a given train  $i$  and stop  $j$ , the actual departure delay  $D_{ij}$  is:

$$D_{ij} = t_{dep_{ij}}^{actual} - T_{timetable_{ij}} \quad (12)$$

where  $t_{dep_{ij}}^{actual}$  is the actual departure time from the station and may or may not be equivalent to  $t_{dep_{ij}}$ , depending on the simulation outcome. It is again remarked that the fact that there are already some departure delays in the base scenario is justified since the train trajectories were computed with an in-house tool and may not be consistent with the official SBB timetables.

It can be observed how if the punctuality is reduced from about 80% to 50% for the S 20 line, whereas it remains consistent at around 70% for line S 30. In the case of line S 30, this is probably due to enough buffer time at the stops to recover the imposed stochastic delays. The trains that were already delayed, however, are severely delayed after including the additional stochastic delays, by an amount much greater than the magnitude of the additional delays themselves. In particular, a high number of trains that were delayed around 200 seconds are delayed between 300 and 600 seconds after including the additional delays, and trains that were previously delayed around 600 seconds are delayed up to 1200 seconds after including the additional delays. This is due to the network affects, and trains being forcibly stopped at points of the networks due to track being occupied by other trains, increasing their delays.

A similar effect occurs with line S 20, which had smaller actual departure delays in the first place. A large amount of trains face delays of between 200 and 400 seconds, with some trains being delayed up to 1200 seconds too. Early departures (due to the studied case with  $\lambda = 1/120^*$ ) can be spotted in the histograms.

Figure 19 shows the power demand profile of trains in the delayed scenario and can be compared with the original power consumption profile plotted in Figure 10. The new profile,

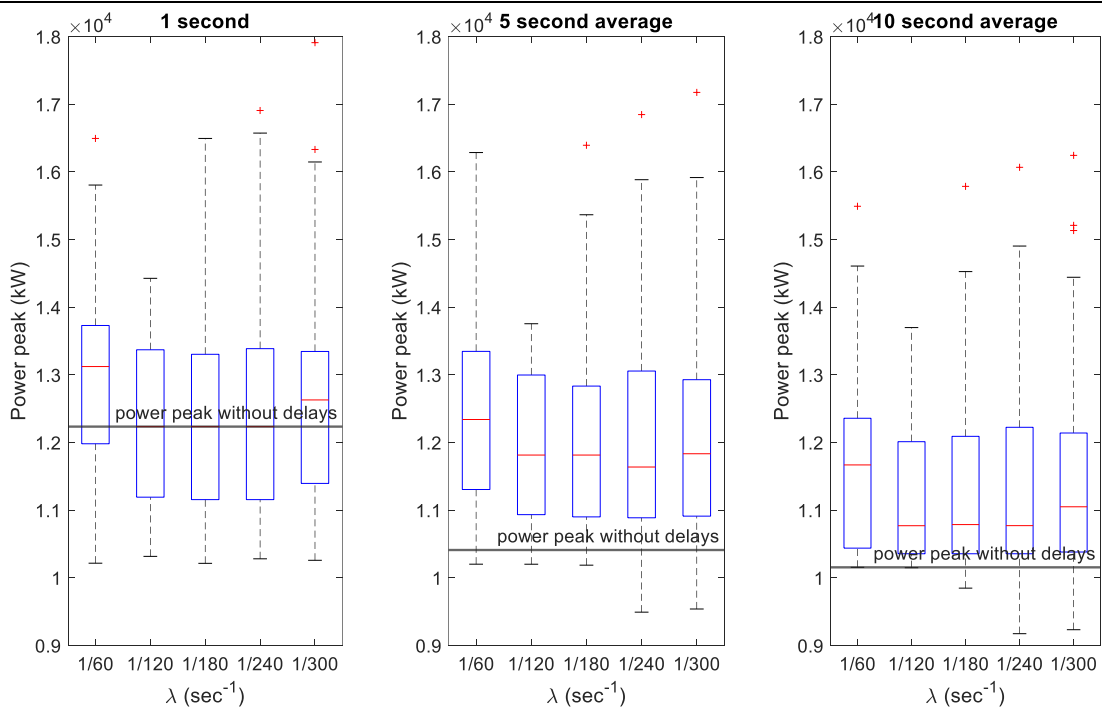
due to the delays and the stochastic effects, shows a less regular structure and the equivalence between the first and second hour of the simulation no longer holds. As a consequence of the stochastic delays, a severely high power peak occurs in minute 90 of the simulation, with a magnitude above 15000 kW. It is important to remark that in order to be able to study the effect of the delays, as well as their propagation and their effect on the power peak, it is vital that the power peak of the original power demand profile is not at the beginning of the simulation horizon, since then there would be no room for the delays to propagate and study their effect.

The new train trajectories corresponding to the delayed scenario are plotted in Figure 20, and can be compared with those of the base scenario included in Figure 12. The trajectories lose all their regularity and patterns. As an example, IR train (number 31) which departs Locarno after minute 75 of the simulation, is stuck behind a severely delayed RE 80 train (number 41) from Tenero to S. Antonino, meaning not only that the IR train is in consequence also severely delayed, but it is also forced to stop at the signals in Gordola and Riazzino (where the train normally does not stop) as well as those signals defining the block sections between Riazzino and Cadenazzo, meaning that the trains faces more braking and acceleration phases leading to higher energy consumption and a greater chance to have a high power peak in the network.

#### **4.2.2 Delay scenario 2**

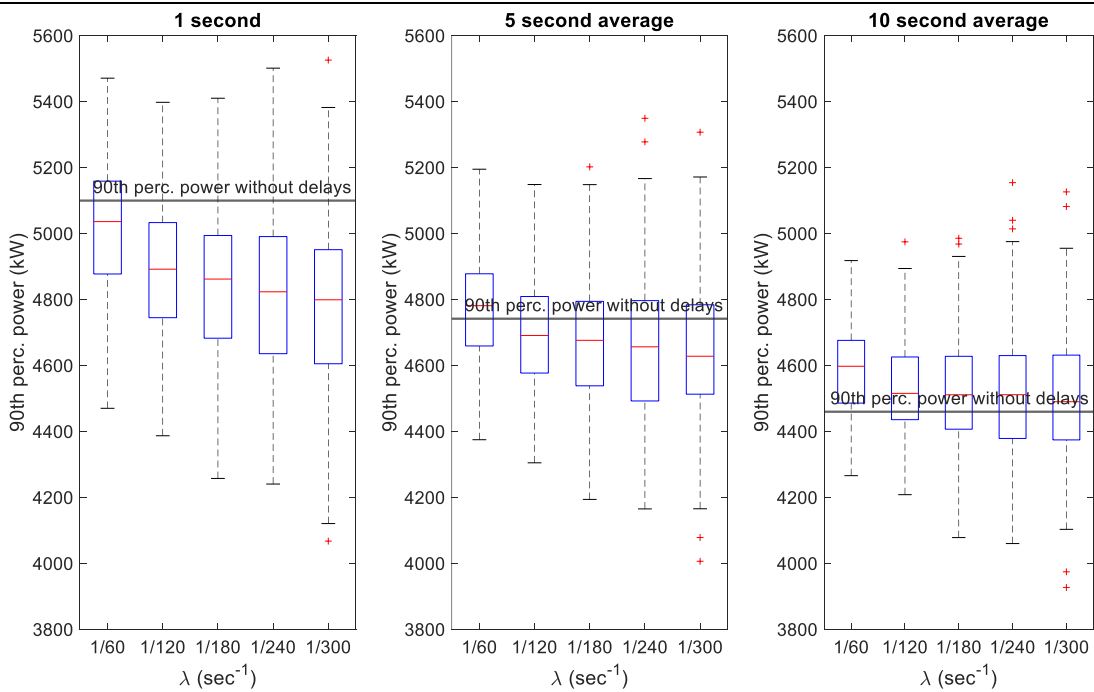
Figures 21 thru 23 present the overall results of the simulations, by showing in the form of boxplots the values for the power peak (Figure 21), 90<sup>th</sup> percentile power (Figure 22) and 50<sup>th</sup> percentile power (Figure 23) when sampling delays with different values of  $\lambda$  ranging from 1/60 to 1/300 seconds<sup>-1</sup>. Greater values of  $\lambda$  are chosen for this scenario since delays are exclusively introduced in the interface. For each case, results considering a 1-second resolution for the power profile, as well as smoothed cases with a 5 and 10-second rolling average are presented, as was done in delay scenario 1.

Figure 21: Results of delay scenario 2 (power peak)

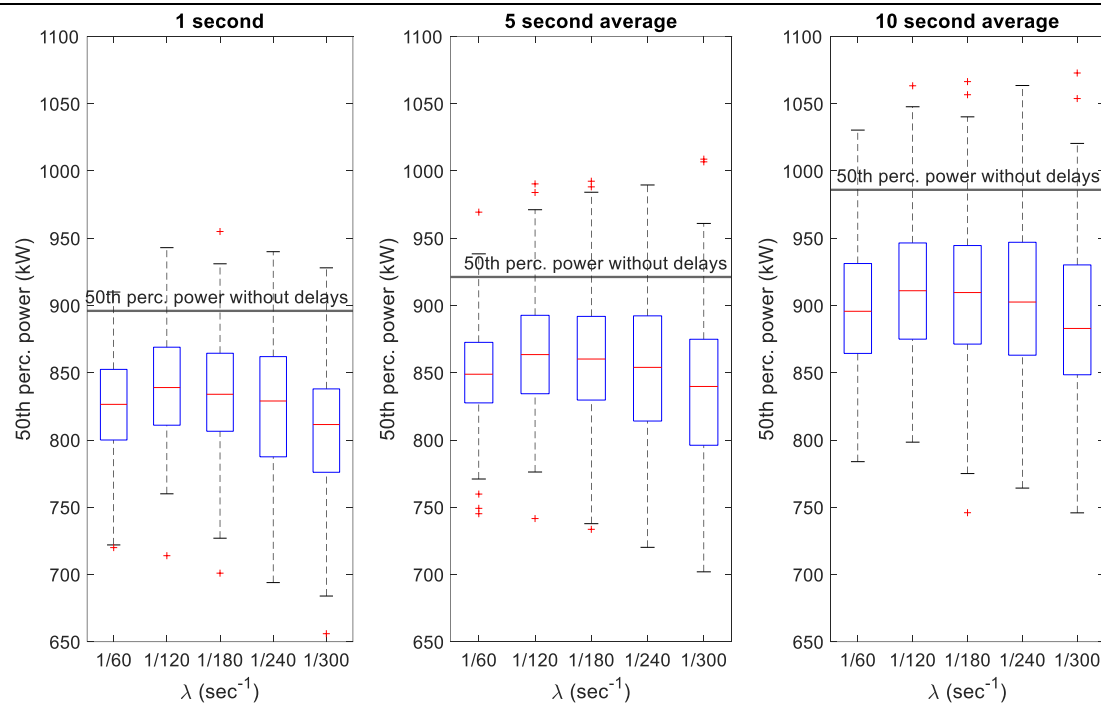


Source: own elaboration

Figure 22: Results of delay scenario 2 (90<sup>th</sup> perc. power)



Source: own elaboration

Figure 23: Results of delay scenario 2 (50<sup>th</sup> perc. power)

Source: own elaboration

The results, in particular those for the power peak as shown in Figure 21, indicate that the delays in the interface have a smaller influence towards the power peaks compared to delaying the trains in every station, as in scenario 1. This happens even when including very large delays in scenario 2, with  $\lambda = 1/300 \text{ s}^{-1}$ .

It is particularly surprising to see that the case with  $\lambda = 1/60$  is the one where the median value for the power peak is higher, independently on whether a 1, 5 or 10-second rolling average is used. Further to this point, when using a 1 second resolution, the median values when the expected delay at the interface is 120, 180 or 240 seconds remains identical to the original power peak. This means that out of the 200 simulations run in each case, a significant amount of them had the same power peak of 12236 kW as in the base scenario. Once again, this is an interesting stochastic effect and the fact that this is not the same when using a 5-second rolling average (median values are clearly higher than in the base case) indicates that the peak in these runs of the simulation was sustained in time for much longer than in the base scenario.

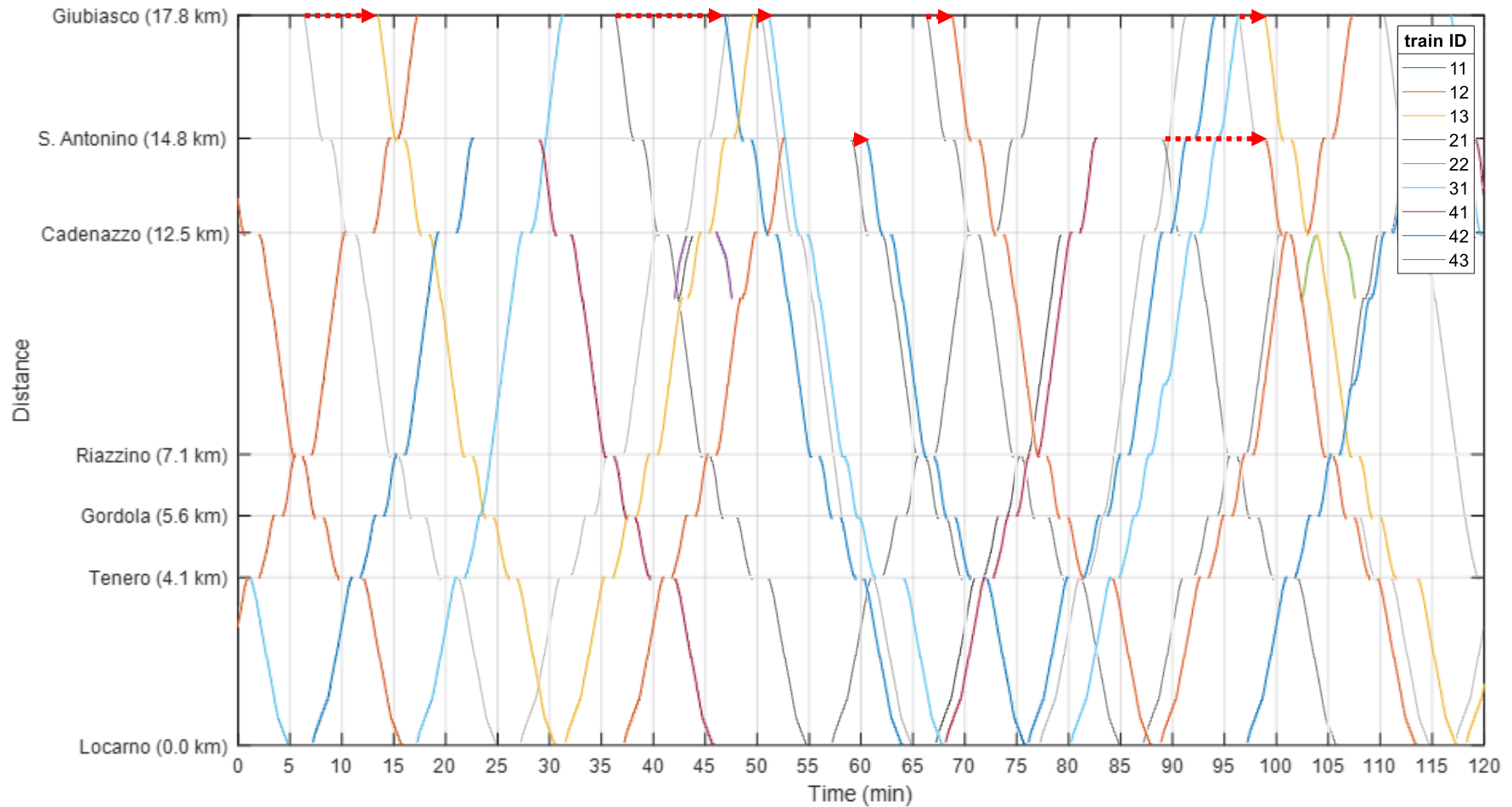
Even though the median values of the power peak show a lower variability when the value of  $\lambda$  increases when compared to delay scenario 1, the outliers do reach high values when  $\lambda$  is increased. This means that although the sensitivity of the power peaks towards the magnitude of delays is not extremely significant, the most extreme cases with the highest peaks do occur with the highest delays. It is also worth pointing out the fact that for  $\lambda = 1/120$  the power peaks are the lowest, meaning that the network effects and interaction between trains occur in some way in the simulation such that when sampling from this delay distribution the tendency towards generating higher power peaks is reduced.

Regarding the 90th percentile power, median values are below the original 90th percentile power without the delays in all cases, other than those computed using a 10-second rolling average. The 90th percentile power tends to decrease as  $\lambda$  increases. The results for the 10-second rolling average show very limited variability between cases, again confirming that a 10-second rolling average provides too much smoothing to the power profile.

In Figure 23, the results show that the 50th percentile of the power is less prone to reaching as low values as those reached in scenario 1 (Figure 17), where instances with a 50th percentile power well below 650 kW were attained.

The trajectories for a particular run of the simulation with  $\lambda = 1/300$  are plotted in Figure 24. The light grey trajectories correspond to the original trajectories as included in Figure 12. Red arrows show the stochastic delays in the interface, as sampled from the corresponding probabilistic distribution. When comparing the new trajectories to those in delay scenario 1 (Figure 20), it can be observed how the timetable still conserves most of its original structure since trains are mostly dispatched in the same way as originally. Figure 24 shows how the train trajectories which are delayed rarely have a big influence on other train trajectories. Furthermore, the available buffer time at the terminal stop (Locarno) is normally sufficient to begin the return journey on time, other than for trains of lines S 20 (train 11, 12 and 13) which have a very small turnaround time in Locarno. Other disruptions can still occur, such as train 41 being delayed as it departs Locarno after minute 65 since arriving train 31 was delayed in the interface and, in consequence, is occupying the last block section before Locarno later than expected.

Figure 24: Train trajectories during the simulation horizon (delay scenario 2).



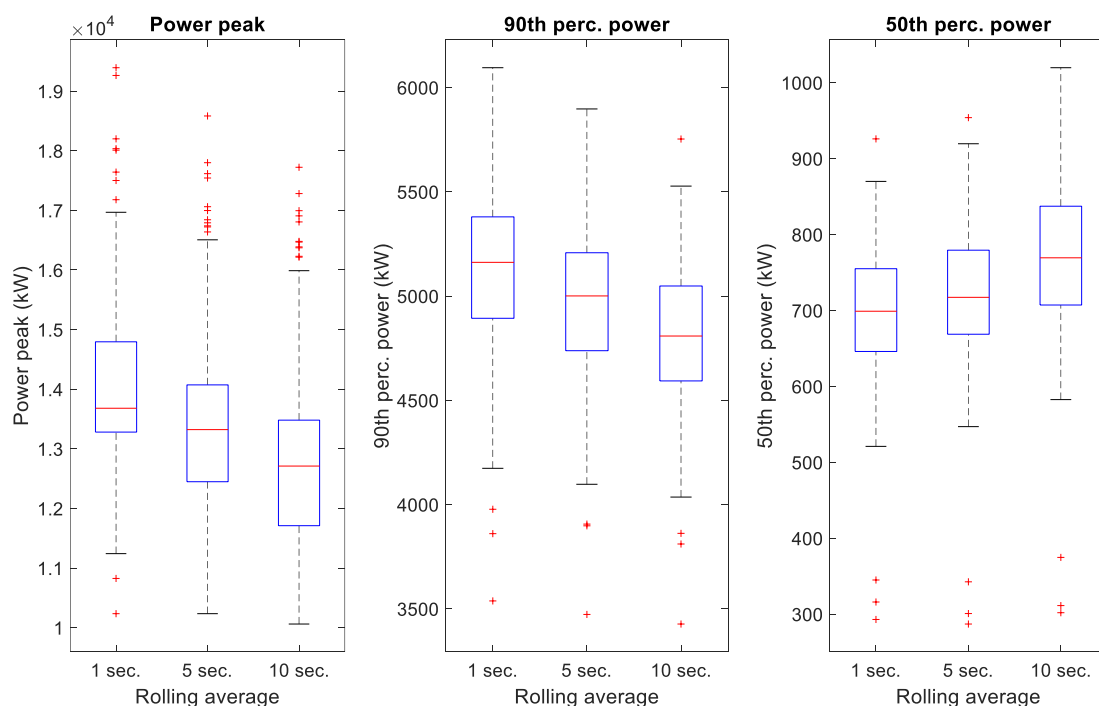
Note: grey lines correspond to the original trajectories without delays. Red arrows show delays in the interface. Source: own elaboration

### 4.2.3 Delay scenario 3

Delay scenario 3 corresponds to the combination of delay scenarios 1 and 2, using the most representative cases of each scenario. For scenario 1, the case with a higher delay is used in combination with the negative time shift ( $\lambda = 1/120^*$ ) since it is considered appropriate to include the case with a possible early departure. For scenario 2, since most of the cases delivered similar results, the higher value corresponding to  $\lambda = 1/300$  is selected because, on the one hand, it delivered the highest peak when analyzing the results with the 5-second rolling average, and on the other hand, it is appropriate when simulating a scenario with very severe disruptions to have even higher delays when the trains interact with the main line in the interface.

Figure 25 shows the outcome of the 200 runs of the simulation.

Figure 25: Results of delay scenario 3

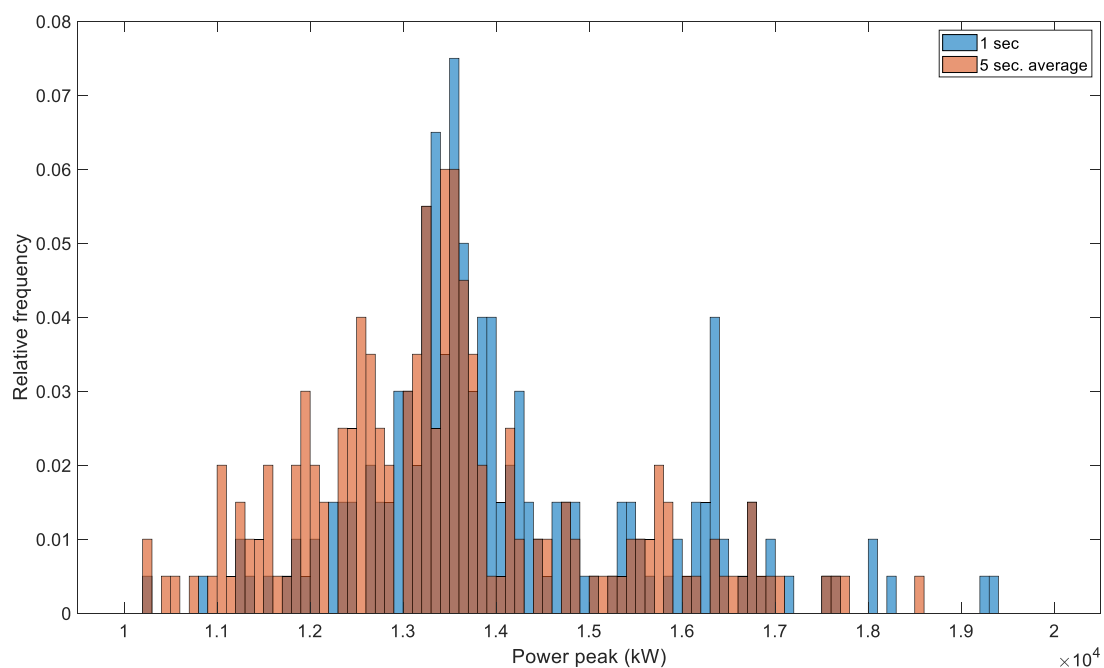


Note: the layout of the figure is different to that in Figures 15 thru 17 and 21 thru 23, since only one case was simulated. Source: own elaboration

The results are very similar to those obtained in scenario 1 with  $\lambda = 1/120^*$  (see Figures Figure 15, Figure 16 and 17) when comparing the median and upper/lower quartile values. However, it must be noted that the inclusion of greater delays in the interface lead to to more extreme points (outliers) with some peaks around 17000 and 18000 kW.

Figure 26 plots in a histogram the frequency of the different magnitudes of the power peak after the 200 runs of the simulation. Bearing in mind the magnitude of the original power peaks without random delays (see Table 4), it can be contrasted how these can increase all the way up to close to 20000 kW when using a 1-second resolution and close to 19000 kW when using a 5-second rolling average. There are two further aspects which are worth highlighting in Figure 26: firstly, the magnitude of the most frequent peaks coincide for both rolling averages; secondly, there is a surprising high frequency for peaks calculated with a 1-second resolution in the bin (16200 kW, 16300 kW). Again, this can only be understood as a consequence of the network and stochastic effects caused by the delays, which make having a 1-second power peak of around 16200 kW to 16300 kW much more likely than any other value between 14300 kW and 20000 kW.

Figure 26: Comparison of power peak distribution in delay scenario 3



Note: power peaks without random delays: 12236 kW (1 sec.) and 10412 kW (5 sec. average).  
Source: own elaboration

#### 4.2.4 Summary of results

The results of all three delay scenarios that have been considered in this work are summarized in Table 5. The table includes indicators (mean value, standard deviation, maximum value and minimum value) regarding the power peak for each of the cases when using a 5-second rolling average to smooth the power demand profile.

Regarding the mean values, the highest are attained in delay scenario 1 with expected delays of 60 and 90 seconds. The mean values in delay scenario 2 are lower than those in scenario 1, for all values of  $\lambda$ . The mean value in delay scenario 3 is just barely above the mean value of scenario 1 for the equivalent scenario.

The variability in all cases is rather low, with coefficients of variation (std. dev./mean) of around 10%. This indicates that the results are fairly homogenous, with the mean values being a representative indicator. Nonetheless, power peaks are generally an extreme phenomenon, and as such, the study of extreme cases is of particular interest. In this regard, the maximum value for a power peak was obtained in delay scenario 1, when using  $\lambda = 1/120^*$ . In consequence, this is the case to be used in the optimization with delay section of this paper (see section 5.4.2). The maximum peak in the case with  $\lambda = 1/90$  also provided a very high power peak, noticeably around 1800 kW higher than the maximum with  $\lambda = 1/60$  and  $\lambda = 1/120$ . In delay scenario 3, the maximum value is surprisingly lower than that of the equivalent case in delay scenario 1, meaning that the inclusion of delays in the interface does not necessarily lead to the highest peak attained throughout all the conducted simulations.

In contrast, the analysis of the minimum power peaks obtained throughout the 200 runs in each case is interesting to grasp whether there is a potential in reducing power peaks by means of controlling trains when they stop at the stations. In four cases, the minimum power peaks recorded were below 10000 kW, suggesting that delaying trains strategically by forcing appropriate additional dwell times at the stations can possibly lead to decreases in the magnitude of the power peaks in a railway network.

Table 5: Summary of results of all delay scenarios for the power peak

Delay scenario 1			Delay scenario 2			Delay scenario 3		
$1/\lambda$ (s <sup>-1</sup> )	Peak power (kW)		$1/\lambda$ (s <sup>-1</sup> )	Peak power (kW)		$1/\lambda$ (s <sup>-1</sup> )	Peak power (kW)	
<b>30</b>	Mean	12313	<b>60</b>	Mean	12242		X	
	Std. dev.	1392		Std. dev.	1220			
	Max.	17907		Max.	16287			
	Min.	9844		Min.	10202			
<b>60</b>	Mean	13106	<b>120</b>	Mean	11918		X	
	Std. dev.	1583		Std. dev.	1140			
	Max.	17603		Max.	13757			
	Min.	9999		Min.	10202			
<b>90</b>	Mean	13602	<b>180</b>	Mean	11867		X	
	Std. dev.	1568		Std. dev.	1187			
	Max.	19412		Max.	16395			
	Min.	10235		Min.	10188			
<b>120</b>	Mean	13617	<b>240</b>	Mean	11904		X	
	Std. dev.	1498		Std. dev.	1350			
	Max.	17651		Max.	16849			
	Min.	10300		Min.	9493			
<b>120*</b>	Mean	13391	<b>300</b>	Mean	11983	<b>120* and 300</b>	Mean	13459
	Std. dev.	1465		Std. dev.	1322		Std. dev.	1584
	Max.	19462		Max.	17176		Max.	18583
	Min.	10188		Min.	9540		Min.	10235

Note: 5 second rolling average used in all cases. 200 runs for each case. Power peak without delays = 10412 kW.

Source: own elaboration

## 5 Simulation-based optimization of train runs and reduction of power peaks

In this chapter, an optimization of the power demand profiles of trains is to be performed in order to reduce the magnitude of the power peak. This is to be performed by *controlling* the trains and implementing operational measures to anticipate and avoid the highest peaks. Two different control measures are considered in this thesis and are explained in the following sections: the modification of the departure time of trains (section 5.1) and the limitation of their maximum traction power (section 5.2).

### 5.1 Modification of the departure time of trains

The modification of the departure time of trains consists in delaying trains at the stations by imposing an additional dwell time (shifting their departure time). Fundamentally, trains are *controlled* once they stop at the stations and are only allowed to depart once the higher power peaks are prevented, ideally.

Train trajectories are not modified by forcing trains to stop at signals in order to delay them there, since more energy would be consumed overall due to the additional acceleration phase required, also leading to a higher probability of facing a power peak when departing from the signal.

The rationale for modifying the departure time of trains lies in the fact that this way it can be prevented that several trains in the network depart from stations at the same time, since it is generally the overlapping of the acceleration phases of different trains that leads to the generation of the power peaks.

For the optimization process, a discrete set of possible *shifting times* is to be defined, indicating the possible times by which the departure of train from a station can be delayed. This choice set will be referred to as  $S$  in this thesis.

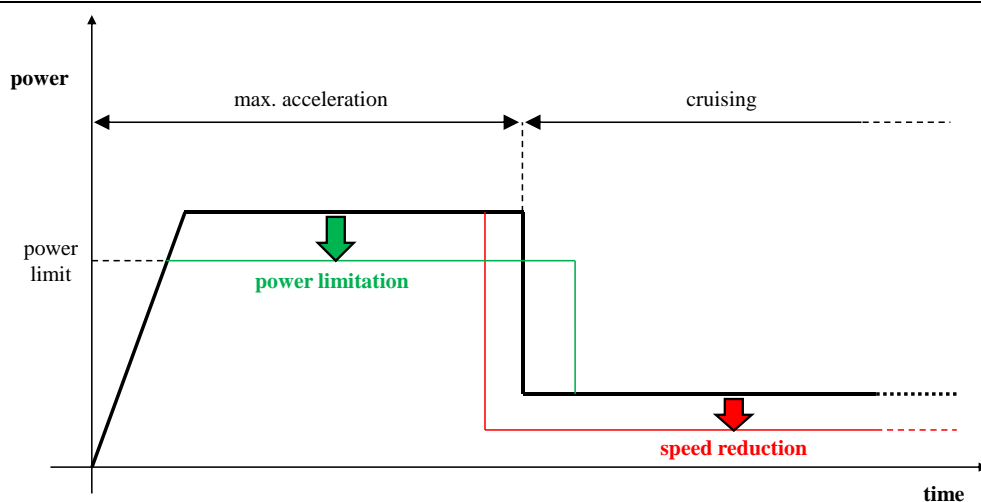
It is important to emphasize that after updating the departure time of train through the sum of the time shift, the new departure might end up not being the actual departure time of train in the case that the following section is occupied by another train at that point in time.

## 5.2 Limitation of the maximum traction power of trains

The limitation of the maximum traction power of trains consists in limiting – in those trains which contribute to the generation of high power peak – their traction power such that they can only use a given percentage of it. In all the cases and results presented until this point, the power limit was always 100%, meaning that trains had all traction power available.

Figure 27 shows the effect of limiting the power of trains and compares it to limiting the speed of trains, which may seem as a more intuitive approach. In terms of power consumption, the effect of reducing the speed of trains only means that the acceleration phase is shortened since a lower speed has to be attained. In contrast, with power limitation, the maximum power which is used during the acceleration phase is limited. The drawback of this limitation is that the acceleration phase has to be extended for longer in order for the trains to reach the target speed of the section.

Figure 27: Difference between power limitation and speed reduction



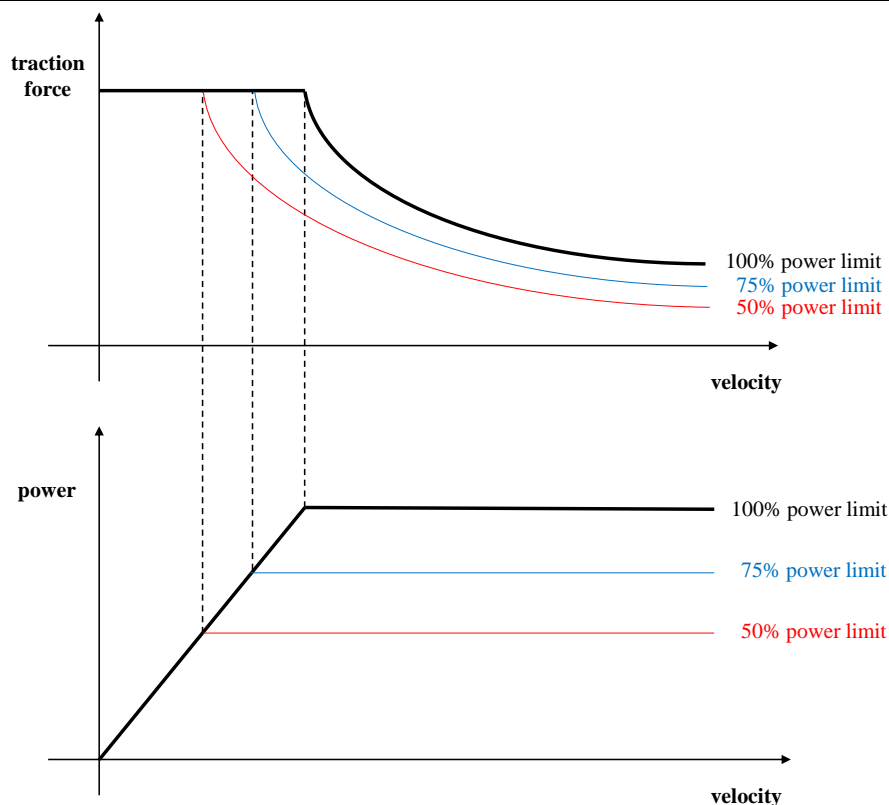
Source: own elaboration

It must be noted that the power limitation approach is valid for regional, Inter Regio and Inter City trains, but would not be applicable for high-speed trains since they typically require their maximum power also throughout the cruising phase.

Other effects of power limitation are shown in Figure 28 by means of the velocity-force and velocity-power diagrams. The velocity-force diagram shows the curves with possible points when trains are fully accelerating and using all power available. It is convenient to recall that

traction power is equivalent to traction force times speed ( $P = Fv$ ). As speed increases, less traction power becomes available. This effect is further emphasized with the limitation of the traction power, for example to 75% or 50% as in the example in the figure.

Figure 28: Power limitation and its effect on the velocity-force diagram

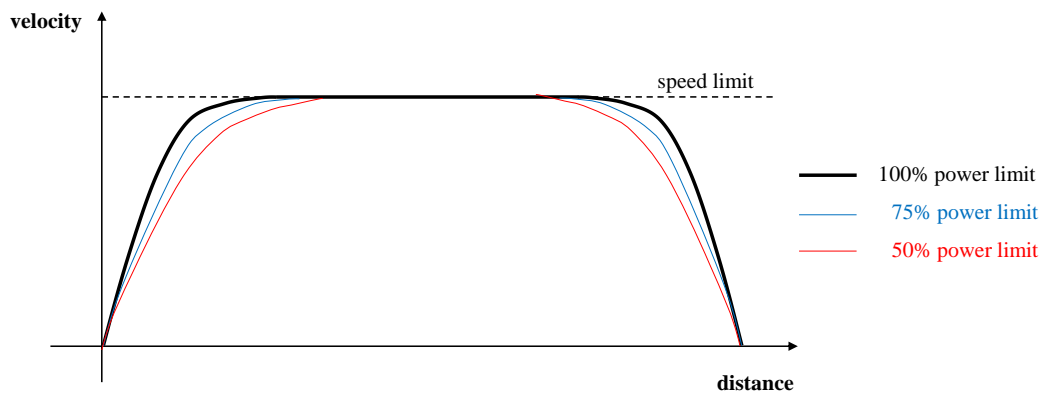


Source: own elaboration

The main advantage that makes power limitation a very convenient approach is that it only increases driving time by a very small margin. Figure 29 shows illustrative distance-velocity diagrams in cases with 100%, 75% and 50% power limitation cases. The different profiles are fairly close between them even when limiting the traction power to 75% or 50%, meaning that driving times for a given section is only increased by a few seconds that can be typically recovered using the available buffer time at the next stop.

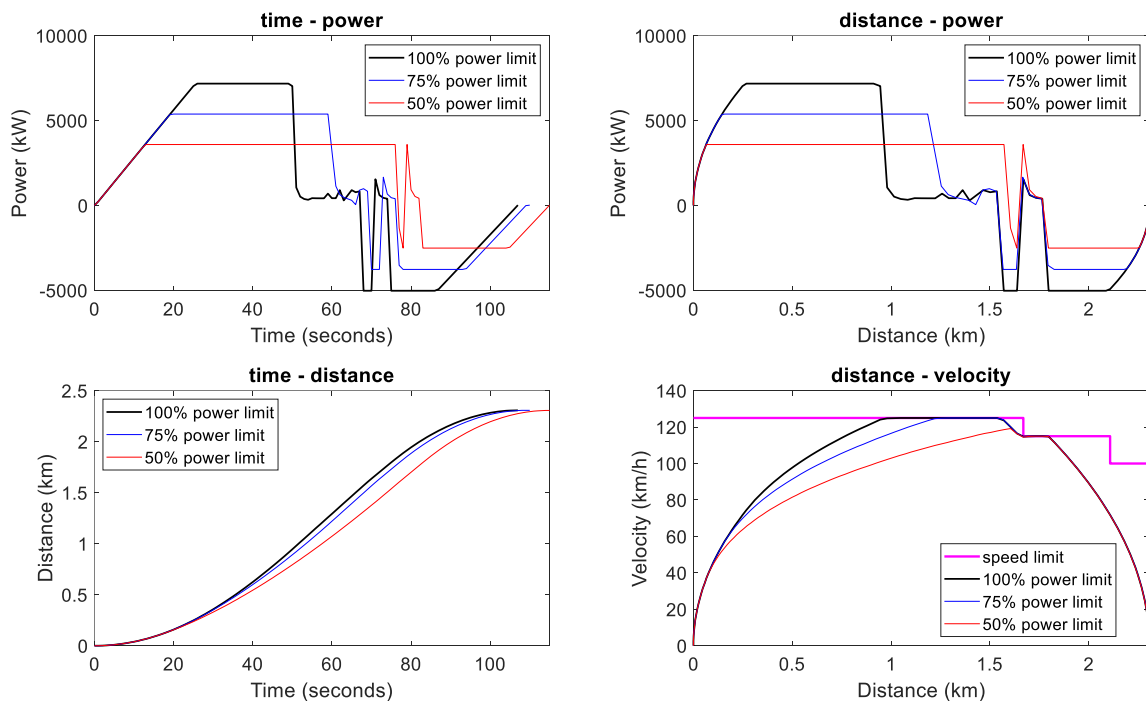
Figure 30 includes an example of 100%, 75% and 50% power limitation using input data from the simulation of the time-power, distance-power, time-distance and distance-velocity diagrams for an IR/IC train running from S. Antonino to Cadenazzo and stopping at both stations.

Figure 29: Effect of power limitation on the speed profiles of trains



Source: own elaboration

Figure 30: Time-power, distance-power, time-distance and distance-velocity diagrams.



Note: IR/IC train in the section between SAN and CD (see Figure 4). The trajectories do not include a coasting phase, since they were computed assuming maximum acceleration and braking conditions. Source: own elaboration from input data.

The time-power plot in Figure 30 shows the extended acceleration phases for the cases with power limitation. Furthermore, the time-distance plots verify how the driving time in the cases with power limitation only increases marginally. Precisely, for this example, the driving

times correspond to 108, 110 and 116 seconds for a 100%, 75% and 50% power limitation, respectively. The distance-velocity diagram shows the speed limit for the section and the different speed profiles. The case with 50% power limitation is not able to reach the maximum speed of 125 km/h in the first part of the section.

Input data has been gathered for this work with power limitations corresponding to cases with 100%, 87.5%, 75%, 62.5% and 50% limitations. Therefore, the available choice set  $L$  for the power limitation of trains corresponds to these values, although it is possible to use only a subset of them. For Inter Regio (IR) trains the lowest allowable power limit is fixed to 75%, due to the irregular stopping pattern of these trains and the fact that they cover long distances without stopping, meaning that a limitation below 75% could be excessive.

As a final remark, power limitations can only be implemented if the target speed (i.e., maximum speed at the end of a section) is achieved, in order to conveniently concatenate different driving schemes (Figure 8) and their corresponding trajectories. In cases that the target speed cannot be achieved with the selected power limitation, the simulation automatically tries with an upper limit until the speed can be attained, eventually reaching 100% power as in the original case.

### 5.3 Optimization procedure

The optimization of the power profile consists in initially determining a maximum allowable power as an objective value (it can correspond with the maximum power capability of the electrical substation, for instance) and then modifying the train runs in a way that all peaks above the objective value are avoided.

For this purpose, every time a train stops at a station it can be controlled by either implementing a time shift to delay its departure, either by limiting its traction power until the next stop or by combining both options.

The drawback of such an optimization is the fact that trains will be further delayed due to the operational measures that are to be implemented. Consequently, it is convenient to minimize the overall delays when conducting the optimization. That is, the objective lies in determining the most efficient control measures to avoid the power peaks while introducing the lowest possible additional delays in the system.

### 5.3.1 Mathematical formulation

Although the optimization problem is to be solved following a simulation-based approach, it is still convenient to write the problem in a formal mathematical way (13) as presented hereunder for the better understanding of the optimization that is to be performed.

$$\begin{aligned}
\text{minimize:} \quad & D = \sum_{i=1}^{n_{trains}} \sum_{j=1}^{n_{stops}} \left( \hat{t}_{dep_{ij}}^{actual} - T_{timetable_{ij}} \right) \\
\text{subject to:} \quad & P_{norm.max} = \max_{T, \Delta_t} \left( \sum_{i=1}^{n_{trains}} P_i(t) \right) \leq P_{objective} \\
& \hat{t}_{dep_{ij}} = t_{dep_{ij}} + t_{shift_{ij}} \quad \forall i, j \\
& P_i(t)_{[j, j+1]} \leq p_{limit_{ij}} P_i^{max} \quad \forall i, j \\
& t_{shift} \in S \\
& p_{limit} \in L \\
& i = 1: n_{trains} \\
& j = 1: n_{stops}
\end{aligned} \tag{13}$$

The objective function to be minimized corresponds to the overall actual departure delays, summed for all trains  $i$  and all stops  $j$ . It is equivalent to that presented in (12) but summed for all trains and all stops here.  $\hat{t}_{dep_{ij}}^{actual}$  corresponds to the actual departure time of a train after updating its expected departure time using the second constraint and adding the time shift. Note again that  $\hat{t}_{dep_{ij}}^{actual}$  corresponds to the first time instance after  $\hat{t}_{dep_{ij}}$  where the section after station  $j$  is available for train  $i$ . In the case of performing the optimization in a case where stochastic delays are considered,  $t_{dep_{ij}}$  would be  $t'_{dep_{ij}}$  instead (9a, 9b).

The third constraint, in turn, corresponds to the power limitation, where the maximum traction power  $P_i^{max}$  of a train  $i$  is reduced according to the desired power limit  $p_{limit_{ij}}$  between stations  $j$  and  $j + 1$ . Note that  $P_i(t)_{[j, j+1]}$  represents the power consumption of train  $i$  between stations  $j$  and  $j + 1$ .

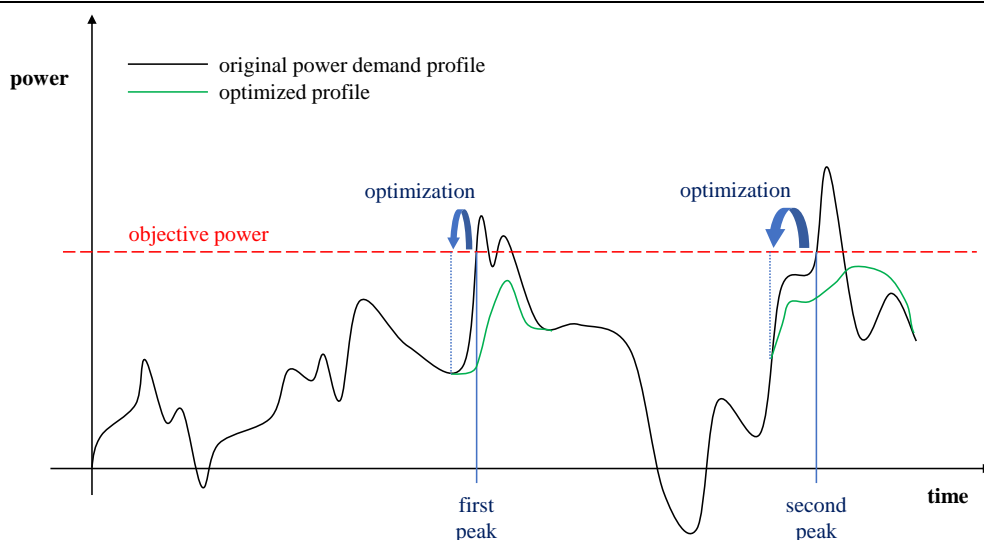
The first constraint includes the condition such that the power peak  $P_{norm.max}$  (2) does not exceed the objective power  $P_{objective}$ . It must be noted that the notation is simplified when referring to trains and station with a single index  $i$  and  $j$ , respectively, since in the simulation the trains of the several lines are numbered differently and the stopping patterns are not the same for all the lines.

The posed optimization problem (13) is also simplified in the sense that the occupancy of sections or the determination of driving schemes are not explicitly included as constraints. In this regard, the developed simulation tool is to be used to be able to capture all the network effects and train interactions accurately.

### 5.3.2 Simulation-based optimization

The optimization problem (13) is to be solved by means of a simulation-based approach. The optimization strategy followed to solve the problem is shown in Figure 31. After initially determining an objective power which cannot be surpassed, the simulation is run for a first time (*prerun*) and the first time instance where the power profile surpasses the objective value is determined. Here, an optimization must be performed by anticipating the power peak and controlling the trains in order to determine a new power profile which shall not exceed the objective power. This is repeated for all other peaks found in the simulation.

Figure 31: Optimization strategy



Source: own elaboration

A flowchart describing the optimization procedure is included in Figure 32. In a first stage, the choice sets  $S$  and  $L$  must be determined as well as the objective power. Then the simulation is run and if any power peak above the objective value is detected, the trains contributing to this peak are determined. In this sense, the time in the simulation when those trains were at a stop before the power peak are determined, in order to be able to control the trains by means of a time shift or a power limitation from this point in time. The number of trains to be controlled is limited to three, so in case that the power peak is caused by more than three trains only the three of them with the highest contribution to the power peak are selected. This is done for the following reasons:

- It is normally a maximum of three trains that contribute to a power peak, and in the cases with more trains, the power contribution of the last trains are typically very low.
- In terms of computational complexity of the optimization process, limiting the optimization to fewer trains has a great positive impact since the number of combinations to be evaluated are much lower. (For example, for  $S(s) = \{0, 15, 30, 45, 60\}$  and  $L(\%) = \{100, 75, 50\}$  there are 15 possible combinations per train, meaning that  $15^3 = 3375$  alternatives must be evaluated if three trains are considered, whereas a total of  $15^4 = 50625$  would have to be evaluated with four trains.)
- From an industry perspective, it is better to modify the least train runs as possible to streamline the train dispatching process.

After determining the problematic trains and evaluation all possible alternatives, the best combination of time shifts and power limitation for each train must be selected. This is done following four priority levels as described below:

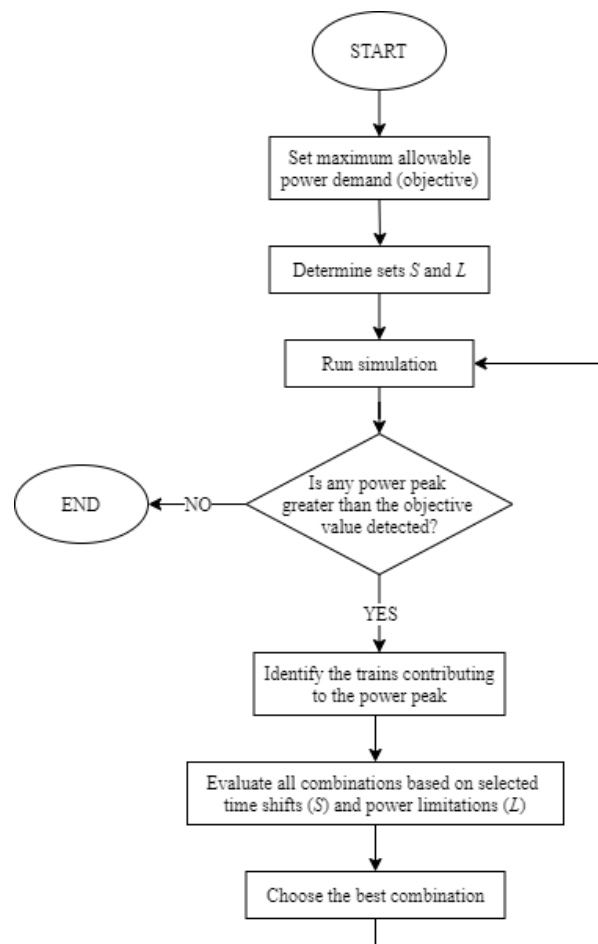
- i. **The power peak must be avoided at the critical time step.** That is, not all the combinations will be able to solve the problematic power peak, so only those which do so are eligible to be selected as the best combination.
- ii. **The next problematic peak should be the furthest away in time.** That is, for each combination, the time step at which the next problematic power peak occurs is determined. Only the combination with the next power peak the furthest away in

time are selected since this way multiple problematic power peaks may be solved at once. This is a positive aspect both from the industry perspective (less train runs are modified) and from a computational perspective (less peak have to be solved).

- iii. **The introduced delay (in terms of power shifts) must be the lowest possible.** That is, the sum of the time shifts assigned to the problematic trains shall be the lowest as to follow the purpose of minimizing the overall delay of all trains.
- iv. **Higher power limits must be prioritized.** That is, it is preferable to not limit the power of trains if the outcome of the optimization remains equivalent.

A heuristic has been developed following the aforementioned priority levels in order to select the best combination in the optimization process.

Figure 32: Flowchart describing the optimization procedure



Source: own elaboration

After determining the best combination, the simulation is run again and in case that further peaks above the objective value are still attained, the optimization procedure is repeated again for the new peaks (Figure 32). Each time that a peak is solved, the corresponding *best combination* of control measures of the trains is saved such that they are applied in the subsequent simulations where the rest of the peaks are to be solved.

As a further indicator of the optimization process, the additional delay due to the optimization ( $\Delta D$ ) is considered (14):

$$\Delta D = D^{optimized} - D^{original} \quad (14)$$

The indicator compares the total actual departure delay of all trains  $D$  as defined in the objective function in (13) between the original and optimized scenarios, meaning that the indicator shows the trade-off in terms of additional delay caused by the power profile optimization process. It must be emphasized that the total delay  $D$  is the sum of the departure delay of each train at each station (15), meaning that if a train is not able to recover from a certain delay (e.g., there is not sufficient buffer time at the stations), this is heavily penalized since the delay is repeatedly summed for each of the stations from which the train departs late.

$$D = \sum_{i=1}^{n_{trains}} \sum_{j=1}^{n_{stops}} D_{ij} \quad (15)$$

## 5.4 Results and discussion

In this section some optimization cases which were performed are presented, with different values for the objective power. Cases are included both without including stochastic delays (subsection 5.4.1) and including stochastic delays (subsection 5.4.2).

In all the cases considered, a 5-second rolling average was used to compute the peaks from the power demand profile.

An i7-10750H processor with 32 GB of RAM memory was used to perform all the optimizations contained in this thesis.

### 5.4.1 Cases without stochastic delays

As an initial case, an **objective power of 10000 kW** is selected. This corresponds to a rather *easy* optimization, since the power peak in the original case is 10412 kW, meaning that the gap between the power peak of the original case and the objective power is relatively small.

Consequently, two different simple optimization cases are implemented. In the first case (optimization 1), a time shift of 15 seconds can be selected, whereas in the second case (optimization 2) the power limit of trains can be reduced to 87.5%. The results of both optimizations are shown in Table 6.

Table 6: Results of the power demand optimization with an objective power of 10000 kW

Case	Original	Optimization 1	Optimization 2
$S$ (s)		{0, 15}	0
$L$ (%)		100	{100, 87.5}
Num. peaks solved		4	4
Num. alternatives computed		24	24
Num. modified trains		4	4
Computation time (s)		40	40
Power peak (kW)	10412	9667	9305
90 <sup>th</sup> perc. power (kW)	4741	4938	4872
50 <sup>th</sup> perc. power (kW)	921	918	934
$\Delta D$ (s)		105	4

Note: 5 second rolling average used when computing the power consumption.

In either case, a total of 4 peaks are solved with the number of alternatives computed being equal in both cases since the number of possible combinations for each train is always two (either do nothing or shift 15 seconds in optimization 1, either do nothing or limit the power to 87.5% in optimization 2). The main difference between both optimization options can be seen in terms of the additional delay caused by the optimization ( $\Delta D$ ). Whereas optimization 2 almost produces no additional delay, the additional delay is significant in optimization 1. It can be verified how the new power peaks are below 10000 kW in both cases, and also how the 90<sup>th</sup> and 50<sup>th</sup> percentile power value change.

Table 7 and Table 8 contain the decision variables (i.e., the resulting time shifts and power limitation of the trains) for each of the optimizations. The tables include the train number, the time in the simulation when the train last stopped at a station before the peak (time at which

the control measure must be implemented) as well as the corresponding time shift and/or power limit to be implemented. The vertical dashed lines separate the decision variables corresponding to the different peaks which are solved. All the trains involved in the power peak are shown in the tables, although it can be verified how its only one of the trains that is modified each time (trains 31, 41, 31 and 43 in both cases).

In this optimization case, the modified trains are the same in both optimizations, with trains that are delayed by 15 seconds in optimization 1 facing a power limitation of 87.5% in optimization 2.

Table 7: Decision variables corresponding to optimization 1

Train ID	13	31	11	21	41	12	31	13	22	43
Time (s)	1501	1650	2435	2371	2384	5101	5250	6035	5970	5984
$t_{shift}$ (s)	0	15	0	0	15	0	15	0	0	15
$p_{limit}$ (%)	100	100	100	100	100	100	100	100	100	100

Source: optimization result

Table 8: Decision variables corresponding to optimization 2

Train ID	13	31	11	21	41	12	31	13	22	43
Time (s)	1501	1650	2435	2371	2384	5101	5250	6035	5970	5984
$t_{shift}$ (s)	0	0	0	0	0	0	0	0	0	0
$p_{limit}$ (%)	100	87.5	100	100	87.5	100	87.5	100	100	87.5

Source: optimization result

As a next step, an optimization with an **objective power of 8000 kW** is performed. Reducing the objective power from 10000 kW to 8000 kW constitutes a sharp change, meaning that the optimization will require a much greater computational effort to provide a solution, as well as larger choice sets both for  $S$  and  $L$ . For this case, five different optimization options are proposed, as can be observed in Table 9.

Optimizations 1 and 2 only involve time shifts, with optimization 2 providing a smaller interval between the different elements (15 seconds). In consequence, the total number of alternatives which must be computed increases from 216 to 800 and in turn, the computation time also faces a sharp increase. Despite the additional computation time, optimization 2 shows some advantages when comparing it to optimization 1, making it worthwhile to have a

larger choice set. On the one hand, one less train is modified (9 instead than 10). Additionally, the total additional delay caused by the optimization is 35% smaller than in optimization 1. This is due to the additional possibilities of shifting trains 15 or 45 seconds, which were not available in optimization 1. Optimizations 3 and 4, in contrast to 1 and 2, rely exclusively on power limitation. Again, optimization 4 provides a broader set of choices when compared to optimization 3, by also including the option to limit the power of trains to 87.5% or 62.5%. For these cases, the results show that there is no real advantage in opting for optimization 4 over optimization 3, since the additional delay is only reduced by a very small margin in optimization with respect to optimization 3 and does not compensate for the additional computation cost. Furthermore, even only 6 peaks are solved in optimization 4 (8 are solved in optimization 3), the number of modified trains is equivalent in both cases.

When comparing optimization 3 with the optimization which rely exclusively on departure time shifting, one can observe how the additional delay is much smaller – even negligible – in the case with power limitation. Finally, a last optimization (number 5) is included by combining time shifting and power limitation and using less restrictive values in both cases (only 15 seconds shift and only 75% as the greater power limitation). The results of this optimization are good in terms of number of modified trains and additional delay, which although higher than the cases with only power limitation, still remains at a very low value. Nonetheless, optimization 5 suffers from the fact that the decisions space is increased with respect to the other optimizations, making the total number of alternatives computed greater. Hence, the computation time rises significantly.

Overall, optimization 3 would be the preferred option unless the railway operator really showed a preference towards minimize the number of train runs to be modified or was reluctant to limit the power of trains as far as 50%. In such case, optimization 5 would be chosen. Table 10 shows some of the decision variables corresponding to optimization 5, corresponding to the first three peaks that are solved. Furthermore, the original and optimized power profiles can be seen in Figure 33, where it can be observed how the power peaks are avoided. The histogram in Figure 34 compares the 1-second power consumption instances between both cases. It can be seen how in the optimized profile the frequency of instances with a consumption around 6000 kW clearly increases. In relation to this fact, the 90<sup>th</sup> percentile power also experiences an increase as can be seen in Table 9.

Table 9: Results of the power demand optimization with an objective power of 8000 kW

Case	Original	Optimization 1	Optimization 2	Optimization 3	Optimization 4	Optimization 5
$S$ (s)		{0, 30, 60}	{0, 15, 30, 45, 60}	0	0	{0, 15}
$L$ (%)		100	100	{100, 75, 50}	{100, 87.5, 75, 62.5, 50}	{100, 87.5, 75}
Num. peaks solved		8	8	8	6	6
Num. alt. computed		216	800	216	750	1296
Num. modified trains		10	9	11	11	10
Computation time (s)		200	690	200	675	910
Power peak (kW)	10412	7940	7831	7971	7773	7773
90 <sup>th</sup> perc. power (kW)	4741	4599	4838	4910	4936	4985
50 <sup>th</sup> perc. power (kW)	921	935	897	940	938	941
$\Delta D$ (s)		1030	665	28	16	127

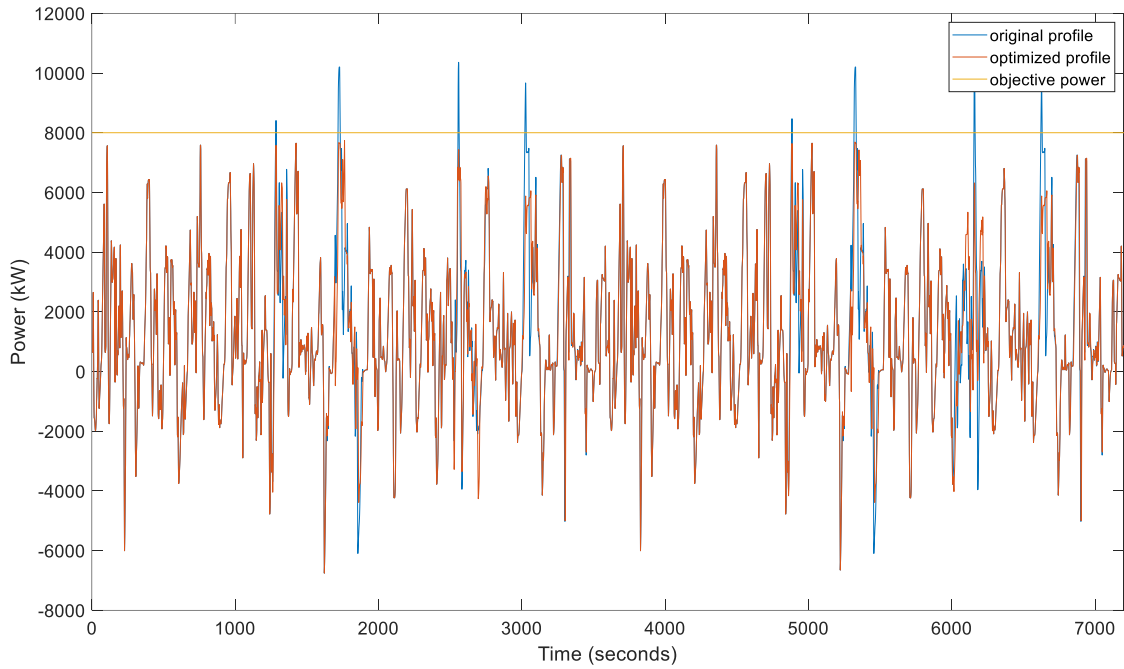
Note: 5 second rolling average used when computing the power consumption.

Table 10: Decision variables corresponding to optimization 5

Train ID	13	22	42	13	21	31	11	41	43	...
Time (s)	1172	1204	1165	1501	1636	1650	2435	2384	2465	...
$t_{shift}$ (s)	0	0	0	0	0	0	0	15	0	...
$p_{limit}$ (%)	100	100	75	75	100	75	100	100	100	...

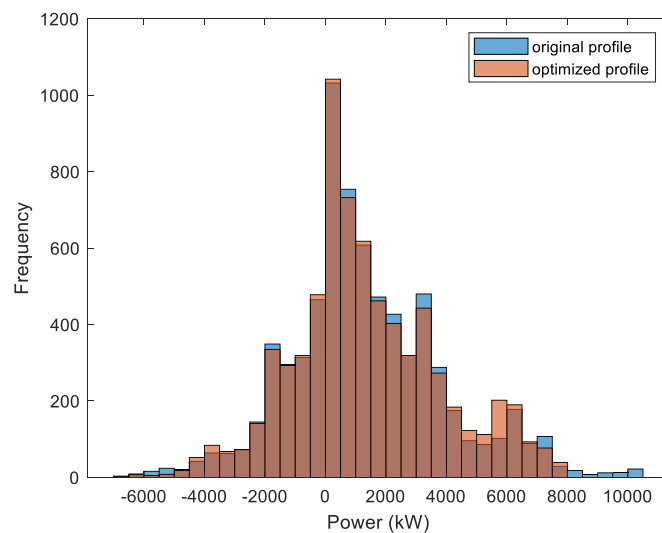
Source: optimization result

Figure 33: Optimized power profile (optimization 5)



Source: own elaboration

Figure 34: Comparison of the power consumption histograms corresponding to the original and optimized power profiles



Note: Objective power = 8000 kW. Source: own elaboration

### 5.4.2 Cases including stochastic delays

When conducting the power profile optimization in cases with stochastic delays, some considerations must be remarked:

- Delay scenario 1 with  $\lambda = 1/120^*$  is considered (see section 4.1).
- The delays cannot be sampled from the given distribution while conducting the simulation, since the same values must be used for each train at each stop in each of the runs of the simulation to be executed during the optimization process (Figure 32). Consequently, a sufficiently long array of delays is sampled at the very beginning, with a vector of delays being assigned to each train. This way, the same delay can be applied to each train in each station during each of the runs of the simulation.
- In the case of shifting the departure time of trains during the optimization, the time shift is to be added on top of the stochastic delay at the station in order to obtain the new expected departure time.

Since different delays are sampled every time, a representative case with an **objective power of 8000 kW** is presented hereunder. The original power peak in this particular optimization instance is of 15935 kW, meaning that the peak power is to be reduced by 50%. Two different optimization options are presented, one relying exclusively on power limitation and one combining power limitation with a possible time shift of 60 seconds. The results of the optimization are shown in Table 11.

Table 11: Results of the power demand optimization with an objective power of 8000 kW (including delays)

Case	Original	Optimization 1	Optimization 2
$S$ (s)		0	{0, 60}
$L$ (%)		{100, 87.5, 75, 62.5, 50}	{100, 75, 50}
Num. peaks solved		15	7
Num. alternatives computed		1675	1152
Num. modified trains		30 (25)	14 (13)
Computation time (s)		1130	880
Power peak (kW)	15935	7925	7991
90 <sup>th</sup> perc. power (kW)	4680	4629	4475
50 <sup>th</sup> perc. power (kW)	906	981	943
$\Delta D$ (s)		227	8419

Note: 5 second rolling average used when computing the power consumption.

Since it does not include any departure time shifts, optimization 1 provides the lowest overall additional delay. The additional delay in optimization 2 is unacceptably high, although it must be remarked that the value corresponds to the sum overall all trains and stops, so the additional delay of specific trains is much lower.

Other than the lower additional delay, no more advantages can be seen in optimization 1 when comparing it to optimization 2. The number of peaks solved in optimization 2 is less than half than in optimization 1, thanks to the 60 seconds departure shifting which allows to solve several peaks in one go, with less operational measures. Consequently, although the decision space is larger in optimization 2, the fewer peaks to be solved means that less alternatives are computed in total and hence, the computation times is lower. However, it must be emphasized that the computation time is still rather high in both cases.

The decision variables corresponding to both optimizations are presented in Table 12 and Table 13, respectively.

Table 12: Decision variables corresponding to optimization 1

Train ID	22	31	43	21	31	42	13	21	31	13
Time (s)	-94	-30	44	1179	299	1369	1344	1179	1521	1754
$t_{shift}$ (s)	0	0	0	0	0	0	0	0	0	0
$p_{limit}$ (%)	100	100	87.5	100	87.5	100	100	50	87.5	62.5
Train ID	21	41	31	43	13	31	43	13	31	43
Time (s)	1913	1844	1865	2985	2961	1865	2985	3149	3205	3088
$t_{shift}$ (s)	0	0	0	0	0	0	0	0	0	0
$p_{limit}$ (%)	100	50	75	50	62.5	87.5	62.5	62.5	87.5	100
Train ID	21	42	43	11	31	41	21	22	41	11
Time (s)	3281	1502	3415	4407	3870	4361	4827	4798	4826	4731
$t_{shift}$ (s)	0	0	0	0	0	0	0	0	0	0
$p_{limit}$ (%)	100	100	50	100	87.5	62.5	100	62.5	50	50
Train ID	31	41	11	12	31	12	31	43	13	31
Time (s)	4921	4826	4731	4969	4921	5124	5288	3633	6560	5288
$t_{shift}$ (s)	0	0	0	0	0	0	0	0	0	0
$p_{limit}$ (%)	87.5	50	50	75	75	87.5	75	62.5	100	75
Train ID	42	31	42							
Time (s)	6410	6805	6810							
$t_{shift}$ (s)	0	0	0							
$p_{limit}$ (%)	62.5	100	50							

Source: optimization result

Table 13: Decision variables corresponding to optimization 2

Train ID	22	31	43	13	21	31	31	43	13	31
Time (s)	-94	-30	44	1344	1179	1522	1920	2985	2960	1920
$t_{shift}$ (s)	0	0	60	0	60	60	0	60	0	0
$p_{limit}$ (%)	100	100	50	100	50	100	75	100	75	75
Train ID	21	31	43	11	12	31	12	22	31	
Time (s)	3038	3205	3141	4765	4969	4920	6575	6420	6803	
$t_{shift}$ (s)	60	60	0	0	60	60	0	0	60	
$p_{limit}$ (%)	75	75	50	50	50	75	100	100	75	

Source: optimization result

In optimization 1, a total of 25 train runs are modified, whereas only 13 are modified in optimization 2. Note that these correspond to the values in brackets in Table 11. The difference with the values without brackets resides in the fact that sometimes, a train is controlled more than once at the same station and at the same time. For instance, in Table 13, train 31 is controlled twice at time 1920 in the simulation, both times imposing a power limitation of 75%. Therefore, instead of 14 trains, its only 13 train runs that are actually modified. In case of a discrepancy between the control measures of a train if it is controlled more than once for a given time in the simulation, the most restrictive measures prevail.

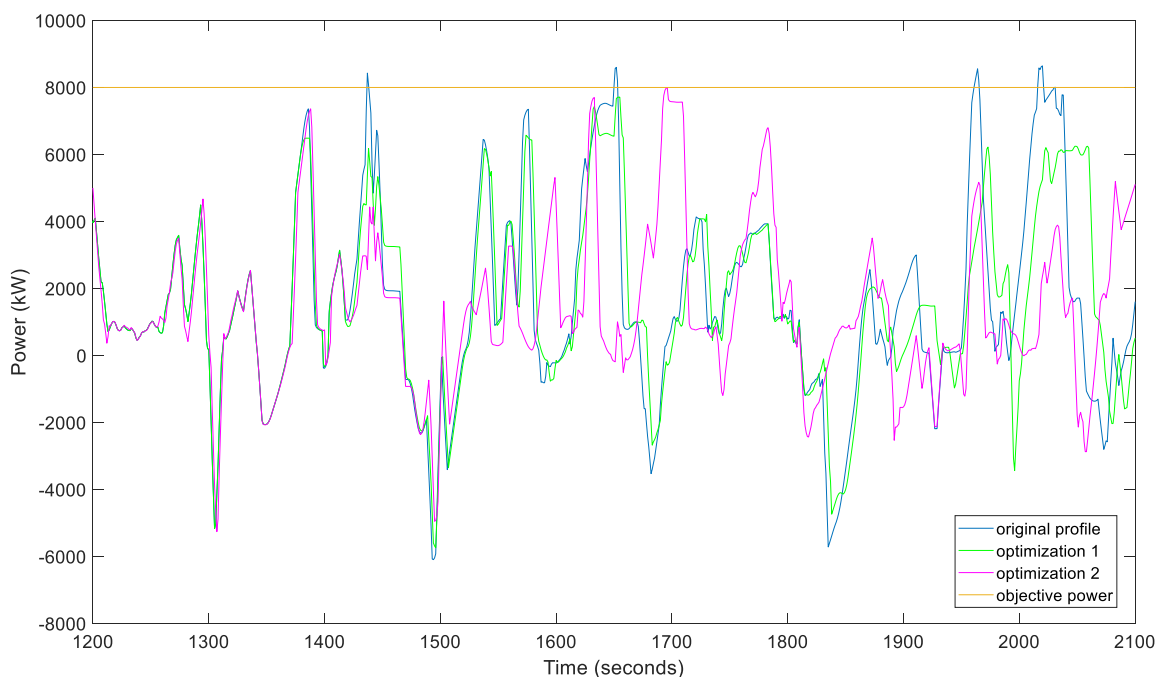
It is important to remark that not all choice sets  $S$  and  $L$  always lead to a feasible solution. That is, for this particular case, having  $S = 0$  and  $L = \{100, 75, 50\}$  did not lead to a feasible solution, and the same happened with  $S = \{0, 30\}$  and  $L = \{100, 75, 50\}$ . Therefore, it was necessary in this case to either refine the power limitation by providing a 12.5% interval in the choice set (optimization 1), or to include a 60-second time shift (optimization 2). Ideally, to prevent infeasible solutions, larger choice sets could be used for  $S$  and  $L$ , but the computation time rises exponentially as already argued. Further to this point, depending on the choice sets used, the objective power and the sampled delays, some optimizations might be unfeasible in all circumstances. For example, it is not viable to further reduce the objective power (e.g., to 6000 kW) since then it is not even possible for two trains to have barely overlapping acceleration phases, and that is not feasible in such a busy network (in particular the line from Locarno to Castione).

Although the power limitation has shown a great potential to reduce the power peaks, the analyzed case here (with stochastic delays) has also shown the usefulness of departure time

shifting, since by including the 60 seconds shifts the overall number of train runs to be modified can be clearly reduced. Again, there is a trade-off between the incurred additional delay and the easiness of implementation from an industry perspective.

Further details of optimizations 1 and 2 can be appreciated in Figure 35, where original and both optimized profiles are compared for a given time frame of the simulation. Whereas in optimization 1 the profile mainly differs from the original one in the sense that around the peaks the consumption is reduced (but conserving the same trend), in optimization 2 the new profile is completely different to the original one, with even the appearance of new peaks. As an example, a new peak just below 8000 kW occurs after second 1700 of the simulation when implementing optimization 2.

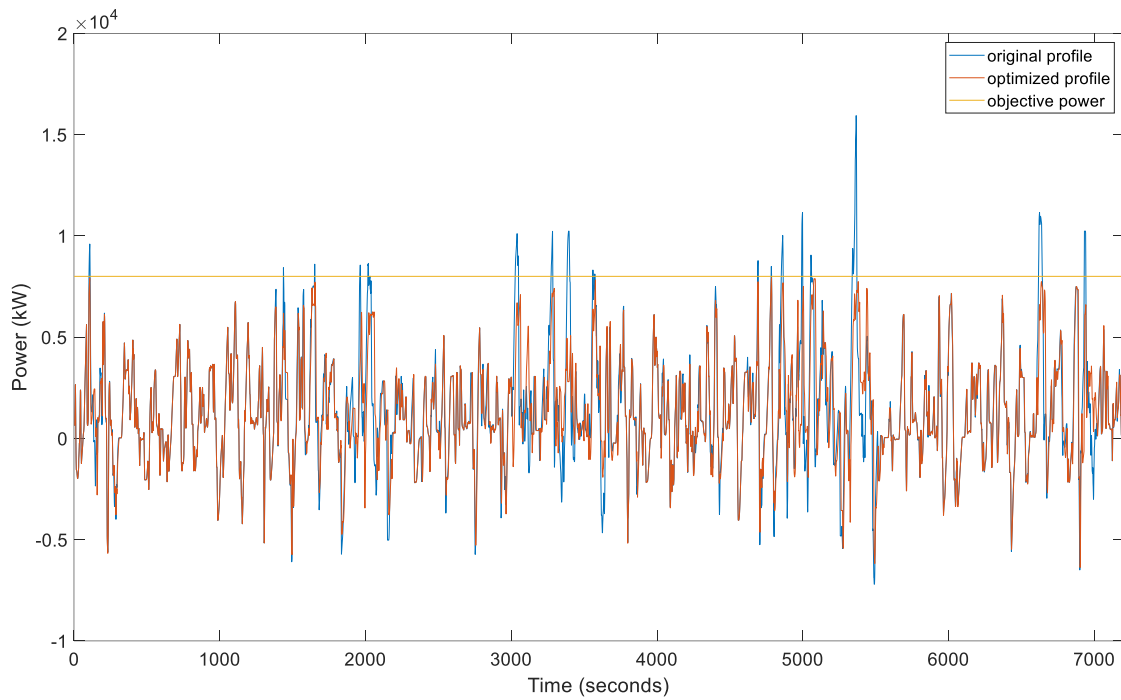
Figure 35: Comparison of both optimized power demand profiles



Note: Objective power = 8000 kW. Source: own elaboration

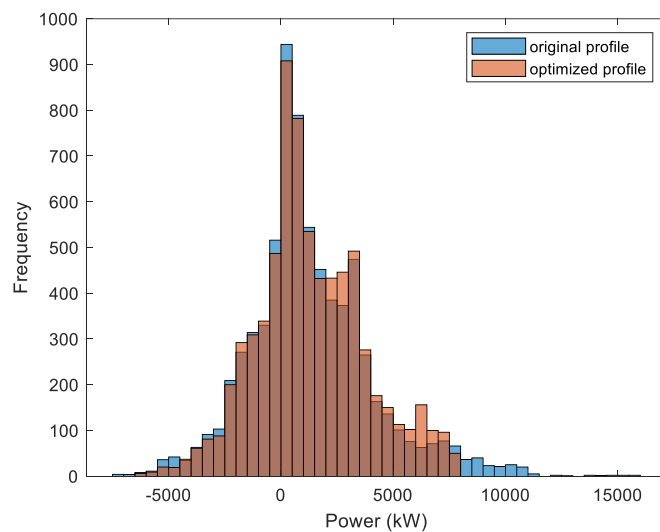
Figure 36 shows the optimized power profile using optimization 1 for the entire time horizon. The histogram in Figure 37 verifies how in the newly optimized profile no power consumption exceeds 8000 kW, and how the frequency of instances between 4000 kW and 6000 kW increases as a consequence of the optimization.

Figure 36: Optimized power profile (optimization 1, including delays)



Note: Objective power = 8000 kW. Source: own elaboration

Figure 37: Comparison of the power consumption histograms corresponding to the original and optimized power profiles (optimization 1, including delays)



Note: Objective power = 8000 kW. Source: own elaboration

## 6 Conclusions and outlook

In this thesis, an efficient event-based simulation tool to quantify the power consumption of trains in a railway network has been developed. The simulation, capable of incorporating stochastic departure delays at the stations, allows to thoroughly study the effect of impunctuality in the power consumption of trains and how the propagation of such delays throughout the simulation horizon can generate extremely high power peaks.

When comparing with the power peaks in the case without any stochastic delays, on average power peaks 30% higher in magnitude occur when including departure delays at every station and 15% higher when implementing the delays only in the interface between the considered power supply and the rest of the railway network. Sampling the delays from a distribution with a higher expected value does not necessarily lead to higher power peaks, since the network effects need to be considered. In this regard, the use of the simulation tool proves to be essential to realistically capture all the inherent network and stochastic effects and correctly model the interactions between trains.

Additionally, the results also indicate that delays can sometimes lead to a slightly lower peak power demand. This suggests that the power peaks can be reduced by strategically delaying specific trains in some stations for a given amount of time. In this regard, shifting the departure times of trains has been combined with the limitation of the traction power of trains in order to optimize the power demand profiles.

The limitation of the traction power of train between two stops has shown great potential as an efficient way to reduce the power peaks. Its major advantage when comparing it to the shifting of the departure time of trains is the fact that it does not generate any significant delays since travel times are only increased by an extremely small margin in most cases. Furthermore, it has been proved how the power limitation approach can also optimize power profiles in situations with stochastic delays, leading in some cases to a reduction of the peak power demand of more than 50%. The great scientific potential of the approach must be contrasted with its applicability. With recent advances towards automated train operation, power limitation can be certainly implemented in the near future, also in driving assistance systems at an earlier stage.

An aspect of the optimization procedure which should be dealt with in the future is the fact that not all combinations should be computed each time a peak has to be avoided. For example, in case that a given combination is already not good enough to be eventually selected, then similar alternatives with higher power limits will definitely not be sufficiently good either, so they should not be computed allowing for the reduction of the overall computational cost of the optimization process. By overcoming this limitation, cases with greater choice sets for both the time shift and the power limitation could be tested.

The other major limitation of the simulation tool consists in the fact that the power limits have to be predetermined before-hand, and the corresponding trajectories have to be prepared as inputs of the simulation. As interesting extensions to be implemented in the simulation for the optimization of the power profile, more power limits could be included (even below 50%) as well as a *best case* consisting in the minimum power for each section such that trains arrive on time consuming all their time buffer. Furthermore, a trajectory optimization module could be ideally included in the simulation and integrated with the power peak reduction.

Other relevant analyses that can be performed using the simulation tool are manifold. The tool offers great flexibility in terms of the definition of the available infrastructure, so analyses concerning the blockage of sections (due to a broken down train or track maintenance) or the upgrading of infrastructure by the opening of new double-track sections and their influence towards the power peaks can be performed. Additionally, although heterogenous traffic has already been considered in this work, it would also be worth including freight trains in the simulation to study their effect. Further studies could involve the investigation of other delay scenarios or experimenting with the modification of any of the other inputs of the simulation, such as the timetable, travel times, dwell times, etc.

## 7 Reference list

- Albrecht, T. (2010). *Reducing power peaks and energy consumption in rail transit systems by simultaneous train running time control*. WIT Transactions on State-of-the-art in Science and Engineering, 39.
- Albrecht, A., Howlett, P., Pudney, P., Vu, X., & Zhou, P. (2016). *The key principles of optimal train control—Part 1: Formulation of the model, strategies of optimal type, evolutionary lines, location of optimal switching points*. Transportation Research Part B: Methodological, 94, 482-508.
- Albrecht, A., Howlett, P., Pudney, P., Vu, X., & Zhou, P. (2016). *The key principles of optimal train control—Part 2: Existence of an optimal strategy, the local energy minimization principle, uniqueness, computational techniques*. Transportation Research Part B: Methodological, 94, 509-538.
- Bärman, A., Martin, A., & Schneider, O. (2017). *A comparison of performance metrics for balancing the power consumption of trains in a railway network by slight timetable adaptation*. Public Transport, 9(1), 95-113.
- Bärman, A., Martin, A., & Schneider, O. (2021). *Efficient formulations and decomposition approaches for power peak reduction in railway traffic via timetabling*. Transportation Science, 55(3), 747-767.
- Bendfeldt, J. P., Mohr, U., & Muller, L. (2000). *RailSys, a system to plan future railway needs*. WIT Transactions on the Built Environment, 50.
- Bergström, A., & Krüger, N. (2013). *Modeling passenger train delay distributions: evidence and implications*. Centre for Transport Studies Stockholm, Swedish National Road & Transport Research Institute (VTI), KTH Royal Institute of Technology, S-WoPEc, Scandinavian Working Papers in Economics.
- Bomhauer-Beins, A. (2019). *Energy Saving Potentials in Railway Operations under Systemic Perspectives*. Doctoral thesis. IVT, ETH Zurich, Zurich.
- Ciccarelli, F., Iannuzzi, D., & Tricoli, P. (2012). *Control of metro-trains equipped with onboard supercapacitors for energy saving and reduction of power peak demand*. Transportation Research Part C: Emerging Technologies, 24, 36-49.
- De la Fuente, E. P., Mazumder, S. K., & Franco, I. G. (2014). *Railway Electrical Smart Grids: An introduction to next-generation railway power systems and their operation*. IEEE Electrification Magazine, 2(3), 49-55.
- Espinosa-Aranda, J. L., & García-Ródenas, R. (2012). *A discrete event-based simulation model for real-time traffic management in railways*. Journal of Intelligent Transportation Systems, 16(2), 94-107.
- Goodman, C. J., Siu, L. K., & Ho, T. K. (1998). *A review of simulation models for railway systems*. In 1998 International Conference on Developments in Mass Transit Systems (Conf. Publ. No. 453) (pp. 80-85). IET.

- Gu, Q., Tang, T., Cao, F., Karimi, H. R., & Song, Y. (2013). *Peak power demand and energy consumption reduction strategies for trains under moving block signalling system*. Mathematical Problems in Engineering, 2013.
- Gupta, S. D., Tobin, J. K., & Pavel, L. (2016). *A two-step linear programming model for energy-efficient timetables in metro railway networks*. Transportation Research Part B: Methodological, 93, 57-74.
- Hill, R. J. (1995). *Electric railway traction. IV. Signalling and interlockings*. Power Engineering Journal, 9(4), 201-206.
- Ho, T. K., Goodman, C. J., & Norton, J. P. (1995). *An event-based traffic flow model for traffic control at railway junctions*. In IRSE International Conference on Advanced Railway Control (ASPECT'95) (pp. 163-170).
- Ho, T. K., Mao, B. H., Yuan, Z. Z., Liu, H. D., & Fung, Y. F. (2002). *Computer simulation and modeling in railway applications*. Computer Physics Communications, 143(1), 1-10.
- Jung, S., Lee, H., Kim, K., Jung, H., Kim, H., & Jang, G. (2013). *A study on peak power reduction using regenerative energy in railway systems through DC subsystem interconnection*. Journal of Electrical Engineering and Technology, 8(5), 1070-1077.
- Khayyam, S., Berr, N., Razik, L., Fleck, M., Ponci, F., & Monti, A. (2018). *Railway system energy management optimization demonstrated at offline and online case studies*. IEEE Transactions on Intelligent Transportation Systems, 19(11), 3570-3583.
- Ko, H., Koseki, T., & Miyatake, M. (2004). *Application of dynamic programming to the optimization of the running profile of a train*. WIT Transactions on The Built Environment, 74.
- Lee, H., Jung, S., Cho, Y., Yoon, D., & Jang, G. (2013). *Peak power reduction and energy efficiency improvement with the superconducting flywheel energy storage in electric railway system*. Physica C: Superconductivity, 494, 246-249.
- Montrone, T., Pellegrini, P., Nobili, P., & Longo, G. (2016). *Energy consumption minimization in railway planning*. In 2016 IEEE 16th International Conference on Environment and Electrical Engineering (EEEIC) (pp. 1-5). IEEE.
- Nash, A., & Huerlimann, D. (2004). *Railroad simulation using OpenTrack*. WIT Transactions on The Built Environment, 74.
- Pankovits, P., Pouget, J., Robyns, B., Delhay, F., & Brisset, S. (2014). *Towards railway-smartgrid: Energy management optimization for hybrid railway power substations*. In IEEE PES Innovative Smart Grid Technologies, Europe (pp. 1-6). IEEE.
- Steiner, M., Klohr, M., & Pagiela, S. (2007). *Energy storage system with ultracaps on board of railway vehicles*. In 2007 European conference on power electronics and applications (pp. 1-10). IEEE.
- Xiao-Ming, X., Ke-Ping, L., & Li-Xing, Y. (2014). *Discrete event model-based simulation for train movement on a single-line railway*. Chinese Physics B, 23(8), 080205.

- Yang, Z., Chen, Y., Zhou, N., & Tong, S. (2019). *PReS: Power Peak Reduction by Real-time Scheduling for Urban Railway Transit*. In 2019 IEEE Sustainability through ICT Summit (StICT) (pp. 1-6). IEEE.
- Yang, L., Li, K., Gao, Z., & Li, X. (2012). *Optimizing trains movement on a railway network*. *Omega*, 40(5), 619-633.
- Yuan, J. (2006). *Stochastic Modelling of Train Delays and Delay Propagation in Stations*. Doctoral thesis. TU Delft, Delft.
- Zhou, Y., Bai, Y., Li, J., Mao, B., & Li, T. (2018). *Integrated optimization on train control and timetable to minimize net energy consumption of metro lines*. *Journal of Advanced Transportation*, 2018.